REVIEW

Aromatic interactions

Christopher A. Hunter,*[a] Kevin R. Lawson,[b] Julie Perkins[a] and Christopher J. Urch[b]

[a] *Krebs Institute for Biomolecular Science, Department of Chemistry, University of Sheffield, Sheffield, UK S3 7HF*
[b] *Zeneca Agrochemicals, Jealott's Hill Research Station, Bracknell, UK RG42 6ET*

Received (in Cambridge, UK) 20th October 2000
First published as an Advance Article on the web 23rd March 2001

Covering: 1950–2000.

1 Introduction

Molecular organisation and molecular interactions are the basis of the functional properties of most molecules, and a detailed understanding of non-covalent chemistry is therefore fundamental to interpreting and predicting relationships between chemical structure and function. Molecular recognition processes are influenced by many different factors which make their study complicated. Progress requires a quantitative understanding of these different factors. Some key functional group interactions, such as H-bonding, are well-understood. H-bonds are strong, single point interactions with a very well-defined geometry, and their magnitude is determined by the electrostatic forces between the donor hydrogen atom and the acceptor atom. For weaker, less well-defined interactions, the picture is not so clear. In this review, we focus on one such class, aromatic interactions. Here there are multiple points of intermolecular contact, the geometry of interaction is variable, and there are a vast range of different functional groups that can be involved. We summarise evidence on the properties of these interactions from a variety of different sources, and we apologise for necessarily omitting related work.

2 Theoretical models

Chemists have known for a long time that mixing some colourless or weakly coloured solutions of certain substances in non-polar solvents gives intensely coloured solutions without perturbing the chemical structures of the molecules. The UV–visible absorption spectrum of the mixture shows bands belonging to the two original compounds and also an additional broad band in the long-wavelength region—a charge-transfer (CT) band. For example, the highly coloured solutions formed from mixtures of aromatic amines and nitrohydrocarbons are attributed to the formation of such CT complexes.

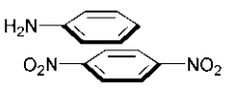

Fig. 1 Proposed structure of the complex between aniline and *p*-dinitrobenzene.

The Mulliken theory is accepted as a valid description of CT complexes.[1] The wavefunction of the ground state of a 1 : 1 complex Ψ_N, is described by eqn. (1), where Ψ_0 describes a no

$$\Psi_N = a\Psi_0(D,A) + b\Psi_1(D^+ - A^-) \quad (1)$$

bond wavefunction and Ψ_1 represents a dative bond wavefunction corresponding to the transfer of an electron from D (donor) to A (acceptor) with weak covalent bond formation. This has been termed an intermolecular electron-pair bond. The ratio b^2/a^2 is generally very small in a molecular complex, but the characteristic CT absorption band is a transition from the ground state ($a^2 \gg b^2$) to an excited state ($a^2 \ll b^2$). The absorption phenomenon which is associated with the exchange of an electron from D to A gives rise to an "intermolecular charge-transfer spectrum".

The conformations of CT complexes can be predicted by consideration of the quantum mechanical symmetry of molecular wavefunctions, or experimentally by studying the dichroism of crystalline complexes.[2] There was little quantitative information about these aromatic complexes available until 1952 when Landauer and McConnell[3,4] presented absorption spectra and equilibrium constants of 1 : 1 complexes formed between aniline and *m*-dinitrobenzene, *p*-dinitrobenzene and trinitrobenzene. From a review of crystal structure data available at that time, the authors put forward a structure for the complexes with the aromatic rings in a stacked arrangement as shown in Fig. 1.

The lack of charge-transfer bands in the UV–Visible absorption spectra of some molecular complexes indicates that there may be another explanation for the formation of these complexes, *i.e.* the CT bands are not related to the mechanism of interaction, rather are a consequence of different intermolecular interactions. If we consider any non-covalent interaction between two molecules, there are several effects to be taken into account: (a) van der Waals interactions which are the sum of the dispersion and repulsion energies. These define the size and shape specificity of the interaction. (b) Electrostatic interactions between the static molecular charge distributions. (c) Induction energy which is the interaction between the static molecular charge distribution of one molecule and the induced charge distribution of the other. (d) Charge-transfer which is a stabilisation due to the mixing of the ground state (AB) with an excited charge-separated state (A^+B^-) as described above. (e) Desolvation: two molecules which form a complex in solution must be desolvated before complexation can occur. The solvent

DOI: 10.1039/b008495f

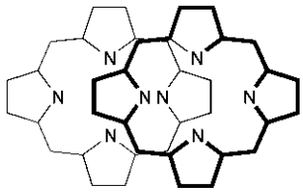

Fig. 2 Stacking geometry in a covalently linked cofacial porphyrin dimer.

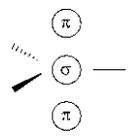

Fig. 3 An sp^2 hybridised atom in a π-system.

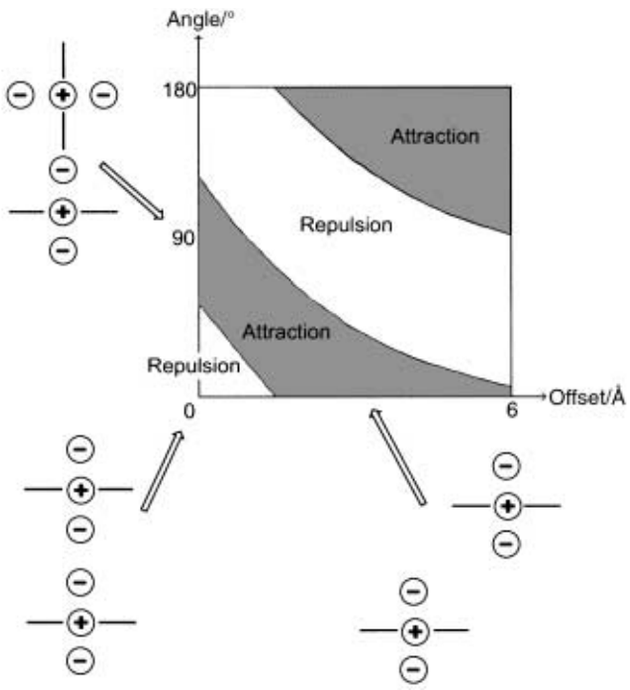

Fig. 4 Electrostatic interactions between π-charge distributions as a function of orientation.

may compete for recognition sites thereby destabilising the complex. Alternatively in polar solvents, solvophobic effects can stabilise the complex.

In order to understand aromatic stacking interactions, it is important to consider the relative effect of each of these forces on the interaction.

2.1 Van der Waals interactions

Aromatic moieties have large planar surfaces, and so a stacked arrangement maximises the van der Waals contacts.

2.2 Electrostatics

In 1990, Hunter and Sanders proposed a model for aromatic interactions.[5] Molecular mechanics calculations on linked cofacial porphyrin dimers consistently predicted a perfectly stacked arrangement of the porphyrin rings, whereas experimental studies show an offset arrangement (Fig. 2). A model of a π-system was proposed with an aromatic ring described as a positively charged σ-framework sandwiched between two regions of negatively charged π-electron density (Fig. 3). The electrostatic interaction between such systems as a function of orientation is summarised in Fig. 4. The term *edge-to-face* will be used to describe the favourable T-shaped, perpendicular arrangement of aromatic rings. *Stacked* describes the non-

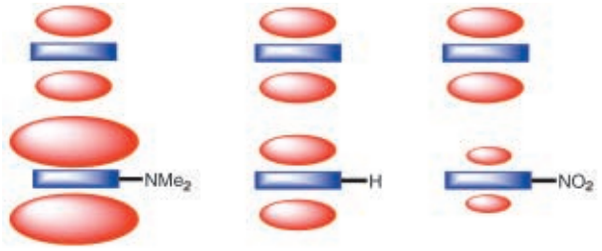

Fig. 5 Schematic representation of the effect of substituents on stacking interactions.

favourable parallel arrangement and *offset stacked* describes the favourable parallel arrangement. This model was used to account for the observed porphyrin stacking geometry. The offset stacked arrangement minimises π-electron repulsion and maximises the attraction between the σ-framework of one porphyrin with the π-electrons of the ring immediately below it.

If the aromatic system is polarised by either a substituent or a heteroatom, stacking interactions can be affected. An electron donating substituent (*e.g.* NMe_2) increases the electron density associated with the ring, therefore increasing the π-electron repulsion. An electron withdrawing substituent (*e.g.* NO_2) has the opposite effect (Fig. 5). A heteroatom in an aromatic ring can be electron neutral, electron rich or electron deficient. When both π-systems are polarised, like polarisations repel and unlike polarisations attract. For unpolarised π-systems the dominant interaction is π-electron repulsion, so an electron deficient π-system stabilises the interaction by decreasing the repulsion.

2.3 Induction

As yet, there is little experimental evidence to suggest that induction effects are important in aromatic interactions. In general, these effects will serve to further stabilise a favourable interaction.

2.4 Charge-transfer

Although charge-transfer bands are commonly observed in aromatic complexes, this is not always the case. Theoretical calculations suggest that these effects make a very small contribution to the stability of the ground state of molecular complexes.

2.5 Desolvation

The flat π-electron surfaces of aromatic molecules are non-polar so that solvophobic forces favour stacking. The hydrophobic effect and the role of the solvent on aromatic interactions will be discussed in detail later.

Following the experimental observation of CT complexes, there were many attempts to model them theoretically. Chesnut and Mosely[6] used partially-extended Hückel theory to calculate the geometries of charge-transfer complexes which agree well with the X-ray crystal structures shown in Fig. 6. A feature common to all the structures is the presence of a π-bond of one molecule approximately centred over and parallel to two edges of a hexagonal ring of the second molecule. Tetracyanoethylene and methylbenzenes were the topic of a different study to calculate the intermolecular interaction energies of the complexes.[7] The "monopoles bond polarizabilities" procedure and a method derived from the semi-empirical treatment were used. Reasonable agreement with experimental data was obtained: the experimental values fall between the two theoretically determined sets of values. The dipole moment of the durene·TCNE† complex, which is generated due to mutual

† The IUPAC name for durene is 1,2,4,5-tetramethylbenzene.

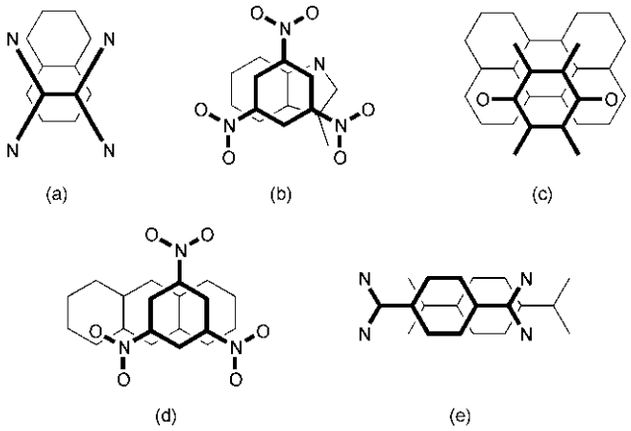

Fig. 6 The arrangements found in X-ray crystal structures of charge-transfer complexes: (a) naphthalene·TCNE (b) skatole·trinitrobenzene (c) perylene·fluoroanil (d) anthracene·trinitrobenzene (e) TCNQ·TMPD.

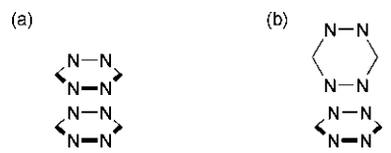

Fig. 7 Geometries of *s*-tetrazine dimers: (a) stacked (b) edge-to-face.

electronic polarisation of the molecules was calculated to be 1.26 D which exactly matches the experimentally determined value.

There have been various attempts to model the benzene dimer theoretically by Linse,[8] Jorgensen and Severance,[9] Jaffe and Smith[10] and Kollman and co-workers.[11] Schlag and co-workers used gas phase *ab initio* techniques and initially predicted an edge-to-face arrangement as the optimum structure with an interaction energy of −6.3 kJ mol^{-1}.[12,13] However, a later study revealed that there are two minima in the potential energy surface of the dimer.[14] The more stable was found to be the offset stacked structure. This structure was also found by Jaffe and Smith.[15] The benzene dimer was studied experimentally using molecular beam spectroscopy, and an edge-to-face dimer was proposed.[16,17] The most stable calculated benzene dimers were also in a perpendicular arrangement. The *s*-tetrazine dimer was studied experimentally by Levy *et al.*,[18,19] and two orientations were observed: stacked and edge-to-face (Fig. 7). The stacked dimer was predicted to be the most stable by calculation, and this geometry agrees well with the experimental data. Price and Stone studied the *s*-tetrazine and benzene dimers and various heterodimers.[20] The Buckingham–Fowler model was used to investigate dimers such as benzene·acetylene, *s*-tetrazine·acetylene, *s*-tetrazine dimer, *s*-tetrazine·benzene, benzene dimer, anthracene·benzene and perylene·benzene. The electrostatic energy was shown to be the dominant force in determining the structures of the complexes.

3 Aromatic interactions in the gas phase

Klemperer *et al.* used the electric deflection of molecular beams to study the benzene dimer.[16] The dimer was found to be polar, and this polarity was attributed to the presence of a permanent electric dipole moment in the ground vibrational state. Therefore the equilibrium geometry of the benzene dimer must be of a symmetry allowing a permanent electric dipole, an edge-to-face geometry. All reasonable geometries in which the planes of the benzene molecules are parallel (stacked) give a non-polar dimer and therefore were eliminated. A coarse study of hexafluorobenzene·benzene identified a stacked arrangement.[17] The

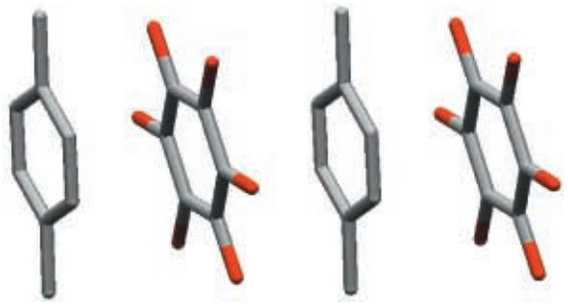

Fig. 8 X-Ray crystal structure of hexafluorobenzene·*p*-xylene.

fluorescence excitation spectra of benzene with perylene and other aromatic species such as anthracene were recorded by Doxtader *et al.*[21] Correlations between potential energy calculations and experimental results suggested that anthracene·benzene adopted an offset stacked arrangement, but benzene was postulated to sit over the centre of mass of perylene. Levy *et al.* also studied the *s*-tetrazine dimer and concluded the rings were in a perpendicular arrangement, but the precise structure was not determined.[22]

4 Aromatic interactions in the solid state

In 1960, a molecular complex between benzene and hexafluorobenzene was reported.[23] Cooling curves of mixtures of the two compounds showed the formation of a 1 : 1 complex which was attributed to charge-transfer interactions. However, no charge-transfer band was found in the UV spectrum. The structure of the complex was determined by neutron diffraction experiments and showed long stacks of alternating benzene and hexafluorobenzene molecules. X-Ray crystal structures of hexafluorobenzene and a series of methylated benzenes have been determined and all show similar interactions to hexafluorobenzene·benzene (Fig. 8).[24]

The formation of such stacks can be explained in terms of the quadrupole moment of the two molecules. The quadrupole moment of benzene is large and negative (-29.0×10^{-40} C m^2), and due to the electronegativity of fluorine, the quadrupole moment of hexafluorobenzene is large and positive (31.7×10^{-40} C m^2). This is represented schematically in Fig. 9. A stacked arrangement of benzene and hexafluorobenzene maximises the electrostatic interaction energy, where a positive quadrupole moment is found parallel and next to a negative quadrupole moment (Fig. 9).

A comprehensive study of the packing patterns of planar aromatic hydrocarbons was carried out by Gavezzotti.[25,26] Geometrically similar molecules crystallise with the same basic packing motif, and there are only a small number of well-defined structural types: herringbone, sandwich-herringbone, sandwich-herringbone β and sandwich-herringbone γ depending on the relative orientation of the molecular planes in the crystal which is reflected in the shortest cell axis. Sandwich-herringbone structures form molecular pairs, which are organised in a herringbone pattern (Fig. 10). Linear correlations of packing energy with the number of valence electrons and molecular surface were obtained. The slopes of both plots were larger than for structures containing heteroatoms, *i.e.* aromatic hydrocarbons form very tightly packed crystals as indicated by a higher packing coefficient (0.748 *cf.* 0.712 for heterocycles). Gavezzotti proposed that the link between molecular and crystal structure is the ability of a molecule to employ C–C and C–H interactions. C–C interactions are optimised in a stacked conformation at van der Waals contact separation and C–H interactions are most effective between edge-to-face molecules. A model for predicting structures was devised based on the number and positioning of C and H atoms in the molecules.[27,28] Part of the molecular surface was defined as stack promoting (core atoms and 50% of the rim carbon atoms) and the rest as

glide promoting (the other 50% of the rim C atoms and all hydrogen atoms). The glide to stack ratio as a function of the total molecular surface provides a predictive map to go from molecular to crystal structure and was used to predict the crystal structures of several hydrocarbons which are not yet known.

5 Aromatic interactions in biomolecules

Aromatic stacking interactions are widespread in nature. The classic example is base stacking in DNA which was first recognised in the structure determined by Watson and Crick in 1953.[29] The melting temperature T_m is the point at which a double helix is 50% dissociated and has been used to determine the effect base stacking has on helix stability. T_m increases with increasing GC content but depends strongly on sequence as well as composition. Helix assembly takes place *via* a co-operative zipper mechanism, where the initial formation of the first few base pairs is an energetically unfavourable process. However once this nucleus is created, new base pair formation leads to favourable contributions to the free energy.[30] Zimm used the theory of melting to try to determine a value for the "stacking free energy"—the free energy gained when base pairs are stacked on each other in the helical arrangement.[31,32] The free energy was estimated to be -29 kJ mol^{-1} per base pair and is therefore the major free energy contribution stabilising the double helix. Interactions between the individual bases and modified bases in aqueous solution have been studied by several groups.[33–35] The general conclusion is that the association of the bases can be largely attributed to stacking of the rings. Solvent effects have also been investigated using the Raman laser temperature-jump technique,[36] again with the conclusion that stacking interactions between the bases dominate the thermodynamics of helix formation. The "dangling end" technique involving an oligonucleotide with a terminal unpaired base has been used in various studies to estimate what one stacking interaction contributes towards helix stability.[37] More recently Guckian *et al.* have looked at aromatic stacking affinities in the context of DNA by substituting the terminal base for aromatic hydrocarbons such as benzene, naphthalene and pyrene.[38] Generally, increasing the size of the aromatic surface increased the melting temperature of the oligonucleotide.

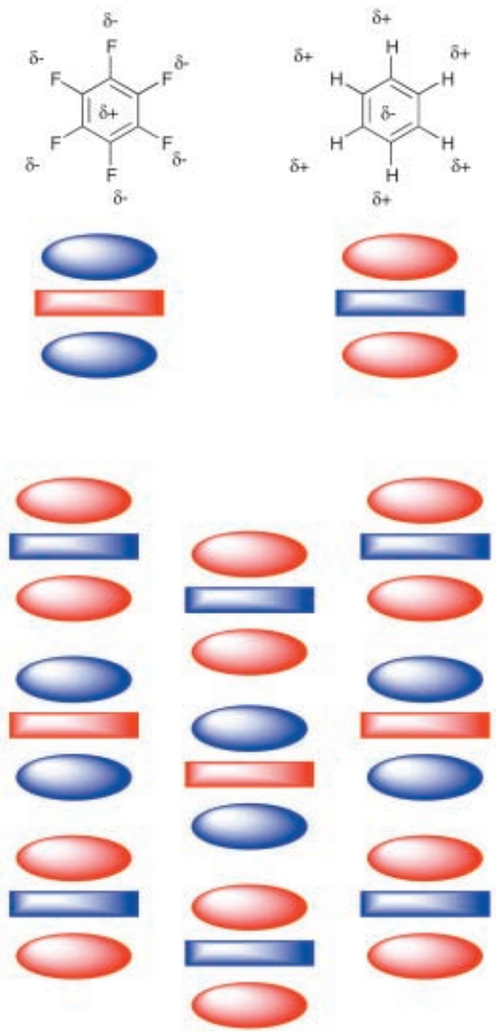

Fig. 9 Schematic representation of the quadrupoles of benzene and hexafluorobenzene, and the arrangement in the crystal which aligns opposite charges.

Nucleic acids play a central role in cellular metabolism and so are a common target for drugs designed to prevent cell replication. Aromatic stacking interactions play a pivotal role in drugs which intercalate with DNA. Intercalation was first observed by Lerman when he studied the complex between DNA and acridine.[39] A mechanism was proposed whereby the acridine could fit between the base pairs of DNA without disrupting the hydrogen bonding motif. This process however causes a change in the physical characteristics of DNA as the helix unwinds, and the bases unstack to allow the intercalator in. This leads to an increase in length of the DNA and a disruption of the regular helical structure (Fig. 11). A variety of DNA intercalators have been found to reduce tumour growth in animals and man, and so these compounds are commonly used as anticancer agents.

In 1985, Burley and Petsko analysed side-chain interactions in proteins.[40] Two aromatic residues were considered to interact if the distance between phenyl centroids was less than 7 Å. The results showed 60 percent of aromatic side chains in proteins were involved in aromatic pairs, and 80 percent of these were involved in networks of three or more interacting side chains. The most favoured distance between the rings was 5 Å, and the most favoured dihedral angle was 90°. Non-bonded potential energy calculations were carried out and showed a typical phenyl–phenyl interaction has an energy of between -4 and

Fig. 10 Packing of naphthalene (HB, left), benzperylene (SHB, middle) and hexabenzocoronene (γ-SHB, right).

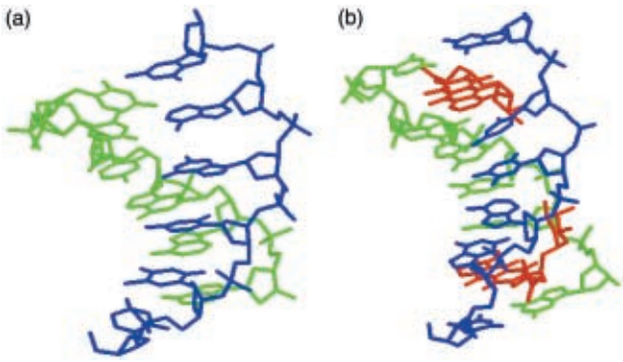

Fig. 11 The DNA double helix in the absence (a) and presence (b) of an intercalator (red).

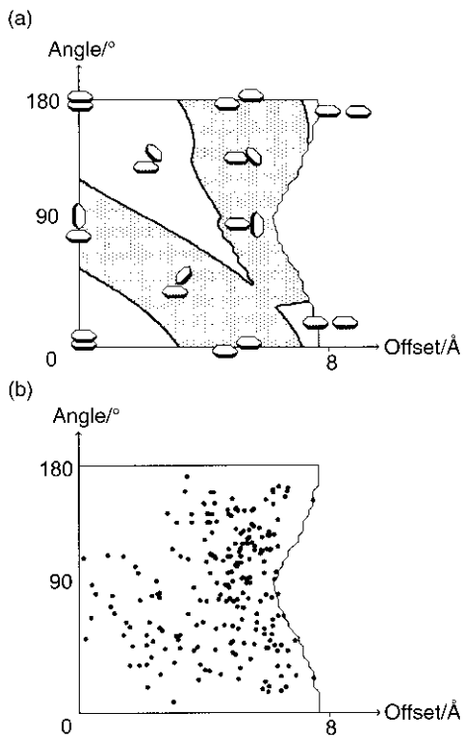

Fig. 12 (a) The electrostatic interaction between two benzene rings as a function of orientation (shaded = attractive, unshaded = repulsive). (b) The geometries of phenylalanine side chain interactions found in protein X-ray crystal structures.

-8 kJ mol^{-1}. The distribution of aromatic rings throughout the protein was also analysed, and aromatic residues and therefore aromatic pairs were not found in regions where the polypeptide chain is disordered. It was therefore suggested that aromatic interactions may form nucleation sites in the protein folding pathway. Hunter calculated the electrostatic interaction between two benzene molecules as a function of orientation and compared it to the observed geometries of interacting phenylalanine rings in proteins with good correlation.[41] The perfectly stacked arrangement was not observed, but a range of edge-to-face and offset stacked geometries were found (Fig. 12).

6 Aromatic interactions in supramolecular chemistry

In the mid 1980s, the concept of supramolecular chemistry, "chemistry beyond the molecule", came into being, and the synthetic molecular receptors which were developed appeared to provide ideal systems for the study of quantitative structure–activity relationships in non-covalent interactions.

6.1 Intermolecular interactions

Ferguson and Diederich studied the complexation of a series

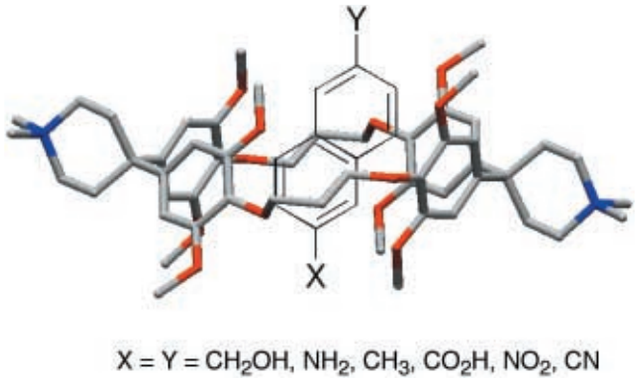

Fig. 13 Cyclophane complexes used to study substituent effects by Diederich.

of 2,6-disubstituted naphthalene derivatives by cyclophanes in d_4-methanol (Fig. 13). The interaction between host and guest was most favourable for guests with electron withdrawing substituents such as X = CO_2H, NO_2 and CN and least favourable for those with electron donating substituents such as X = CH_2OH, NH_2 and CH_3.[42] The cyclophane can be thought of as a donor host with 4 phenyl rings substituted with electron donating methoxy groups. The most stable complexes were formed with electron poor guests, and this suggests that electrostatic interactions are the major factor determining the stability of the complexes. No charge-transfer bands were observed in the UV–visible absorption spectra, indicating CT played no part in the stability of such complexes. This work demonstrated the importance of electronic complementarity in the complexation of aromatic guests. Guests prefer the axial arrangement since this allows highly solvated polar substituents to poke out into the surrounding solvent minimising any unfavourable desolvation. Analysis of the complexation induced shifts of the protons of the guest implied that naphthalene molecules bearing electron accepting substituents are located more deeply within the cavity than those with donor substituents. The experiments were repeated in d_6-dimethyl sulfoxide and the same trends in complexation strength were observed which suggests the differences between guests are not due to solvent effects.

The effect of solvent on aromatic interactions was also studied by Smithrud and Diederich using the complexation of pyrene by a different cyclophane (Fig. 14).[43] The association constants were determined in 18 solvents of differing polarities. A linear relationship was obtained between the stabilities of the complexes and the solvent polarity described by the empirical $E_T(30)$ parameter. Diederich's model describes the solvent properties which appear to be most important in determining the strength of apolar host–guest complexation. Binding is strongest in polar solvents possessing low molecular polarisability and high cohesive factors. Solvents with high cohesive interactions interact more strongly with "like" bulk solvent than with the apolar surfaces of the host and guest molecules, so when complexation takes place, free energy is gained upon the release of surface-solvating molecules to bulk solvent. Thus water is the best solvent for apolar binding.

Whitlock *et al.* designed a macrocyclic host to bind nitrophenol (Fig. 15), $K = 9.6 \times 10^4$ M^{-1}.[44,45] A combination of aromatic stacking interactions and hydrogen bonding was responsible for tight binding. Use of a more flexible linker reduced the binding constant to 6×10^3 M^{-1} indicating the importance of preorganisation.

Dougherty and co-workers used the system shown in Fig. 16 to examine the contributions of aromatic and ion-quadrupole interactions to complexation in aqueous media.[46] Hosts **1** and **2** have similar dimensions and comparable degrees of preorganisation. The rigid framework ensured the charged groups could not interact with the guests, and therefore any difference

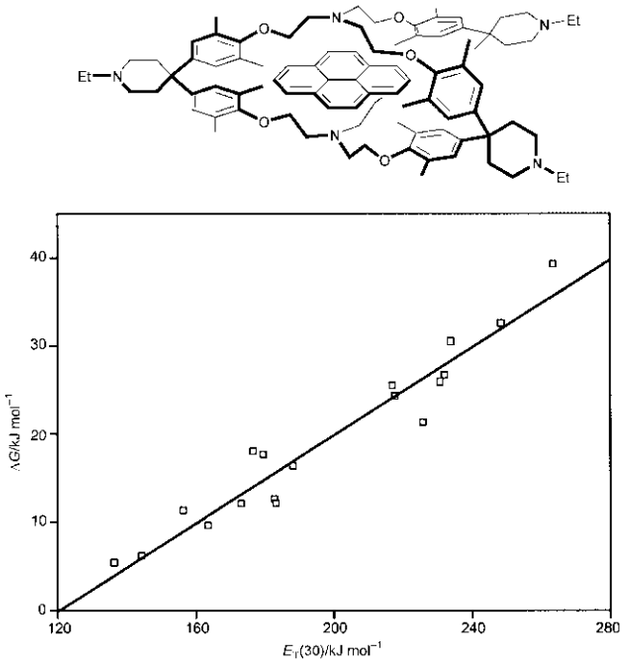

Fig. 14 Dependence of the free energy of complexation of the cyclophane·pyrene complex, $-\Delta G$ (kJ mol^{-1}), on the solvent polarity, $E_T(30)$ (kJ mol^{-1}).

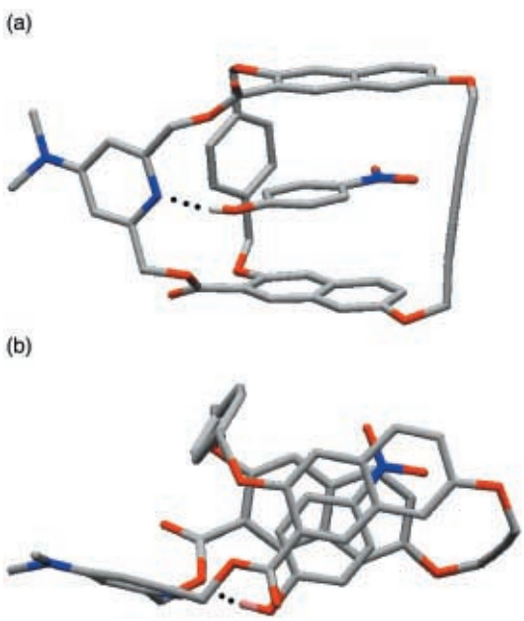

Fig. 15 Two views of the complex formed between Whitlock's bicycle and *p*-nitrophenol.

in binding could be ascribed to interactions with the spacer group. If the hydrophobic effect was dominant, then the cyclohexyl derivative should show the strongest binding (cyclohexyl is more hydrophobic than phenyl). The phenyl derivative should be a better host, if aromatic interactions are important. The results of binding studies are summarised in Table 1.

Both hosts bind the electron deficient quinoline and isoquinoline units **3**–**7** more strongly than the electron rich indole units **8** and **9**. This was evidence that electrostatics play an important role in the binding. The phenyl host **1** bound the charged guests **10** and **11** more strongly than the cyclohexyl derivative **2**. Comparison of the results for isostructural guest pairs showed this enhancement was due to charge and not to steric or hydrophobic effects. The enhanced binding of cations **10** and **11** by the phenyl host **1** was therefore due to the interaction of the positive charge with the π-electrons: the cation–π effect.

Table 1 Association constants K (M^{-1}) for Dougherty's cyclophane hosts with guests **3**–**11** in aqueous solution at 295 K

	K/M^{-1}	
Guest	Phenyl host **1**	Cyclohexyl host **2**
3	1.0×10^4	2.2×10^4
4	1.1×10^4	2.0×10^4
5	3.8×10^4	3.0×10^4
6	4.7×10^4	4.6×10^4
7	5.5×10^4	1.0×10^5
8	1.4×10^3	1.6×10^3
9	2.1×10^3	3.8×10^3
10	4.0×10^5	4.7×10^4
11	2.0×10^5	2.7×10^4

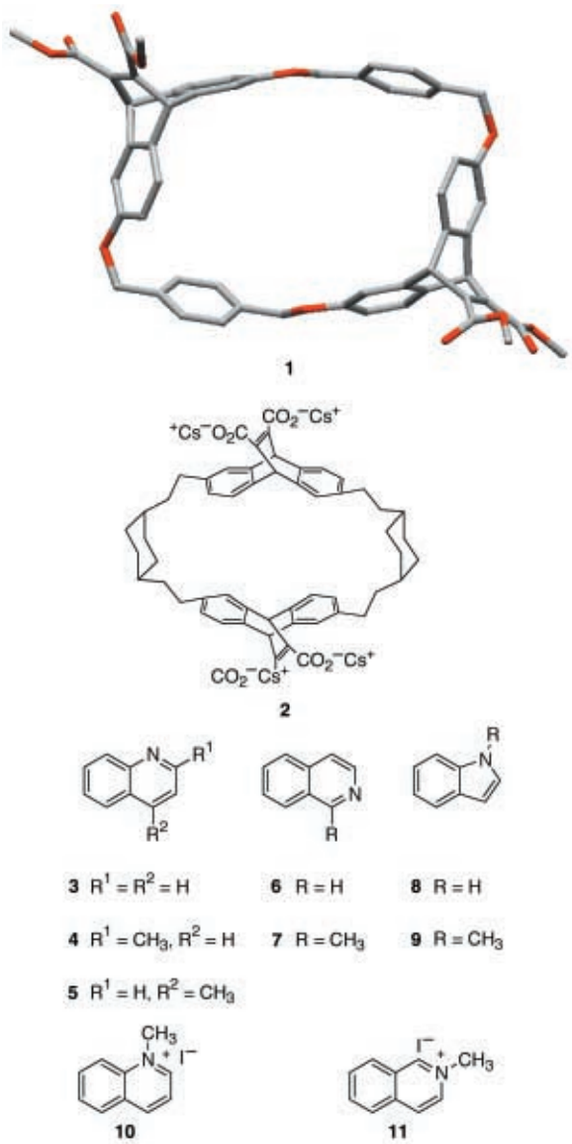

Fig. 16 Dougherty's phenyl host **1** (X-ray structure) and cyclohexyl host **2** which bind guest molecules **3**–**11** in water.

The directionality of the cation–π effect was studied by Schwabacher and co-workers.[47] The cationic **12** and anionic **13** hosts in Fig. 17 were designed to study the interaction of charges with the edge of a bound aromatic ring. Schneider and co-workers had previously shown enhanced binding of aromatic guests by cationic cyclophanes over anionic analogues.[48] The association constants for dihydroxynaphthalenes **14** and

Table 2 Association constants K (M^{-1}) for guests **14**–**17** with Schwabacher's cyclophane hosts

	K/M^{-1}			
	Cationic host (**12**)		Anionic host (**13**)	
Guest	D_2O	D_2O–CD_3OD (60 : 40)	D_2O	D_2O–CD_3OD (60 : 40)
14		7	526	25
15		3	204	18
16	23	10	164	36
17	67		1282	

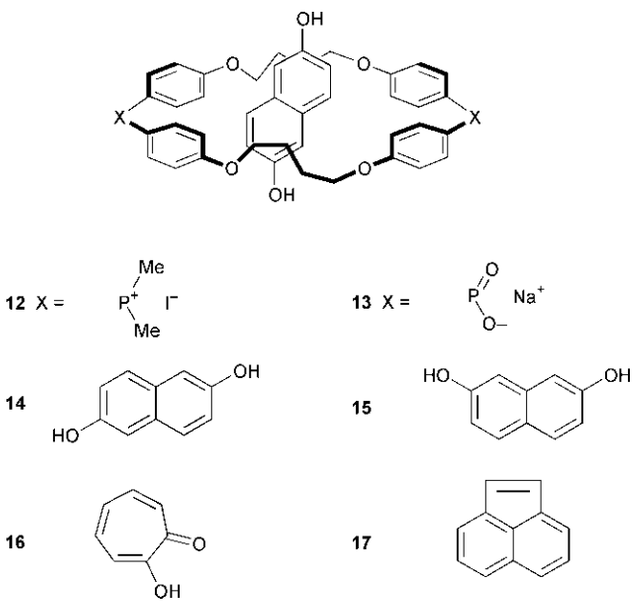

Fig. 17 Schwabacher's cationic (**12**) and anionic (**13**) cyclophane complexes and aromatic guests **14**–**17**.

15, tropolone‡ **16** and acenaphthalene **17** are shown in Table 2. The association constants are larger for the anionic host which implies that the positive edge of the guest interacts more favourably with the negative walls of the anionic host. With the larger aromatic guests tropolone **16** and especially acenaphthalene **17**, where the edge of the aromatic ring is much closer to the charged junction, significant increases in association constants were observed.

In 1987, Hamilton and co-workers reported the synthesis of a class of thymine receptors which showed edge-to-face or stacked aromatic interactions depending on the electronic properties of the substituents.[49,50] Macrocycle **18** formed a 1 : 1 complex with 1-butylthymine **20** ($K = 570$ M^{-1} in chloroform). NMR studies indicated a stacked geometry which was confirmed by an X-ray crystal structure (Fig. 18(a) and 18(c)). MNDO calculations on 2,7-dimethoxynaphthalene-3,6-dicarboxylic acid and thymine indicated a precise alignment of five pairs of oppositely charged atoms (Fig. 18(d)) which confirmed the importance of complementary electrostatic interactions in face-to-face stacking. Tetraether macrocycle **19** bound more weakly ($K = 138$ M^{-1}). MNDO calculations indicated a mismatch in the charge distributions for this system, and NMR spectroscopy and the X-ray crystal structure showed that an edge-to-face interaction is used to avoid stacking (Fig. 18(b)).

Rebek and Nemeth designed a molecular cleft (**21**) to bind aromatic guests (Fig. 19).[51] The binding of **21** to heterocyclic diamines was studied using ^1H NMR spectroscopy. For pyrazine **22**, the binding constant was 1.4×10^3 M^{-1} in chloroform. Quinoxaline **23** showed a 15-fold enhancement in binding ($K = 2.3 \times 10^4$ M^{-1}), due to a stacking interaction with the anthracene group which was revealed by upfield shifts of the quinoxaline protons.

Rebek *et al.* later developed a synthetic system that can recognise adenine using Watson–Crick or Hoogsten hydrogen bonding and aromatic interactions (Fig. 20).[52] Kemp's triacid formed the basis of the receptor which could be substituted with a variety of aromatic groups of varying size and electronic

‡ The IUPAC name for tropolone is 2-hydroxycyclohepta-2,4,6-trien-1-one.

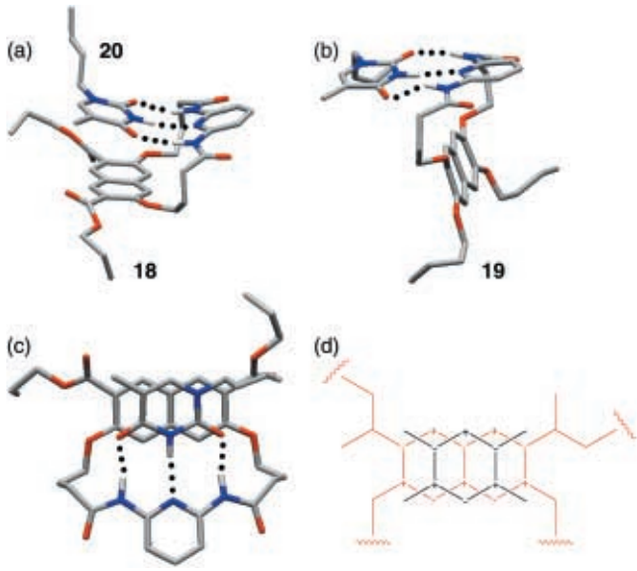

Fig. 18 Hamilton's thymine receptors. (a) Ester substituents lead to a stacking interaction. (b) Alkoxy substituents prevent stacking. (c) The geometry of the stacking interaction in (a). (d) The alignment of charges which leads to the attractive interaction in (a).

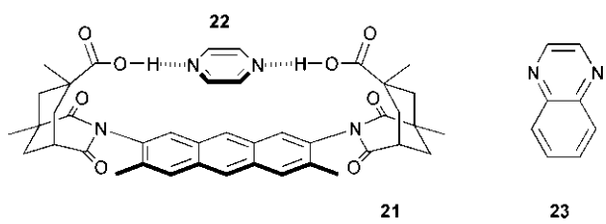

Fig. 19 The complex formed between Rebek's cleft **21** and pyrazine **22**.

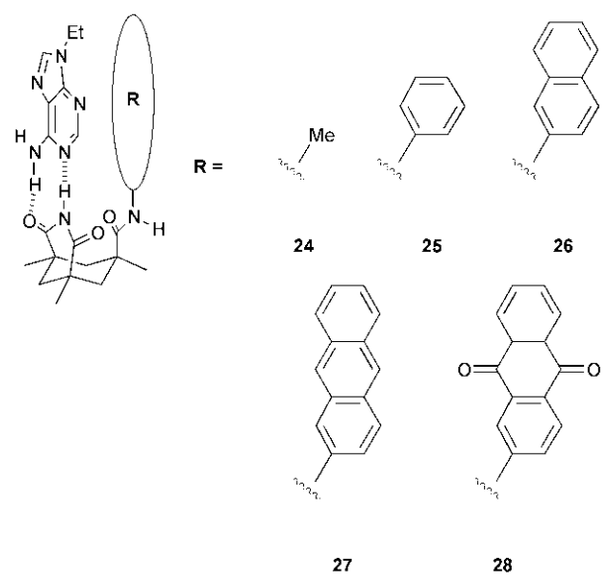

Fig. 20 Complexes used to investigate stacking interactions with adenine.

Table 3 Association constants for complexation of adenine by hosts **24**–**28** in chloroform at 298 K

	24	**25**	**26**	**27**	**28**
K/M^{-1}	75	100	120	440	240

properties. The results of NMR binding experiments are summarised in Table 3. The phenyl and naphthalene systems show only a small increase in the association constant compared to the control methyl amide, whereas anthracene shows a nearly six-fold increase in binding constant which corresponds to a stacking interaction of 4.2 kJ mol^{-1}.

Chen and Whitlock first defined molecular tweezers as synthetic receptors containing two complexing aromatic chromophores connected by a single spacer.[53] Bisfunctional derivatives of caffeine **29** showed an increase in association constant relative to simple caffeine derivatives when complexed with planar aromatic guests such as 2,6-dihydroxybenzoate and 1,3-dihydroxy-2-naphthoate (Fig. 21).

Since then, molecular tweezers have been the subject of an extensive study by Zimmerman. In 1987, he described a molecular tweezer in which a rigid spacer enforced a *syn*-cofacial arrangement of two acridine chromophores as shown by the X-ray structure in Fig. 22(a).[54] The spacer holds the chromophores approximately 7 Å apart, ideal for a planar aromatic guest. Complexation studies were carried out in chloroform solution by ^{1}H NMR spectroscopy, and the tweezer shown in Fig. 22(a) binds 2,4,7-trinitrofluoren-9-one (TNF) with an association constant of 172 M^{-1}. Large upfield shifts observed for the TNF resonances suggest the TNF carbonyl is directed towards the spacer. Both the mono- and di-acridine control compounds **34** and **35** showed association constants of less than 5 M^{-1} with TNF, indicating both acridines are required and that the rigidity of the spacer plays an important role (Fig. 22(c)). Electron donor–acceptor effects were probed using the tweezers **30**–**33** and the results are shown in Table 4 (Fig. 22(b)).[55] As the electron density of the host π-system increases, the association constant increases. The

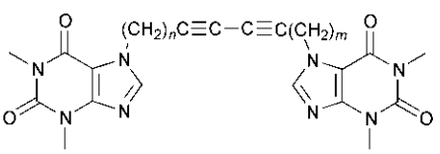

Fig. 21 Whitlock's molecular tweezer.

Table 4 Association constants K (M^{-1}) for complexation of TNF by molecular tweezers **30**–**33**

	K/M^{-1}		
Compound	$CDCl_3$	d_8-THF	$C_4D_8O_2$
30	149	28	47
31	320		
32	475		
33	697		

use of donor solvents, THF and 1,4-dioxane, which solvate TNF better than chloroform greatly reduced the association constants.

Zimmerman and co-workers covalently linked the tweezers to silica to construct chemically bonded stationary phases for HPLC.[56,57] The retention times of several nitro-substituted polycylic aromatic hydrocarbons were measured. The HPLC chromatogram in Fig. 23 shows how increasingly electron-poor aromatics are retained longer on the column. With such good separation, this system was proposed as a potential tool for analysing nitro-polyaromatic hydrocarbons, an important class of environmental pollutants. Good correlation of HPLC and solution enthalpies were obtained with these systems. The tweezer motif is still being used by Zimmerman *et al.* to organise dendritic systems.[58]

Nolte and co-workers used hydrogen bonding and aromatic interactions to design a series of molecular clips.[59] Separation of the effects of hydrogen bonding and aromatic interactions on the binding of resorcinol derivatives was carried out by synthesising a series of clips with different numbers of aromatic

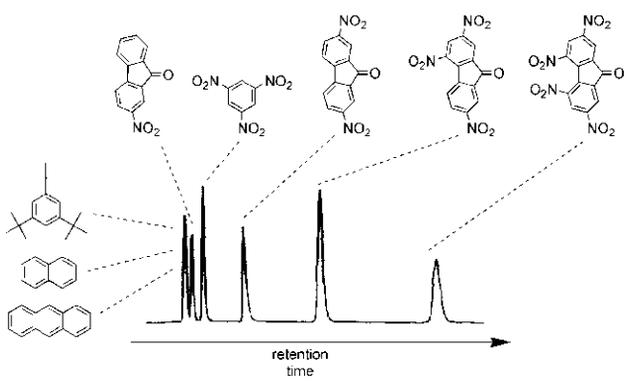

Fig. 23 HPLC chromatogram for a tweezer functionalised stationary phase compound.

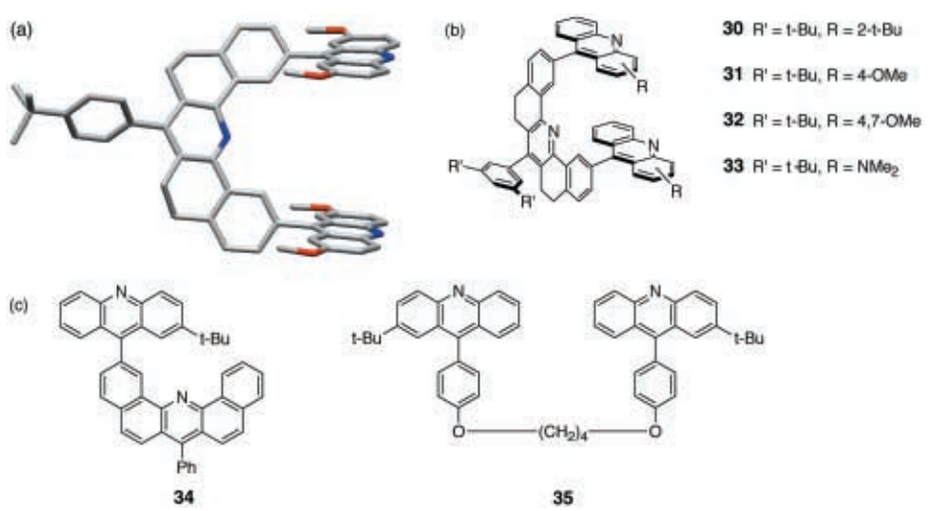

Fig. 22 (a) X-Ray structure of Zimmerman's molecular tweezer. (b) The structures of tweezer derivatives **30**–**33**. (c) Control compounds **34** and **35**.

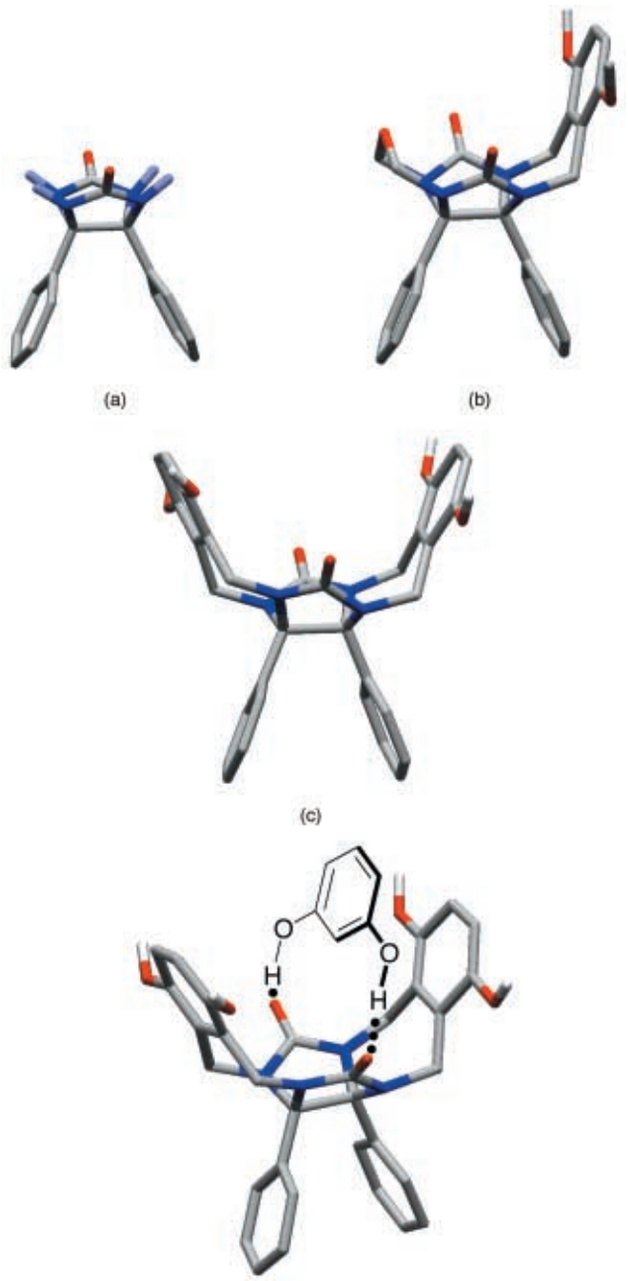

Fig. 24 Nolte's molecular clips and the complex formed with catechol.

side-walls (Fig. 24).[60] The host with no walls can only bind resorcinol by hydrogen bonding ($K = 25$ M^{-1}). With one cavity wall, the association constant increased to 65 M^{-1}, but a second wall dramatically increased the association constant to 2600 M^{-1}. Changing the methoxy substituent on the cavity walls to a methyl group and then to a hydrogen decreased the association constants, and the differences were attributed to a decrease in the strength of the aromatic stacking interaction. Naphthalene side-walls were introduced in an effort to increase the van der Waals contacts between the host and guest. However, this decreased the association constants, presumably due to an increase in the π-electron repulsion between host and guest, indicating it is electrostatics rather than van der Waals forces which play the pivotal role in determining the magnitudes of the aromatic stacking interactions here.

A cleft type receptor for aromatic acids was reported by Crego *et al.* (Fig. 25).[61] The receptor **36** relies on stacking interactions and hydrogen bonding and binds a variety of substituted aromatic acids and amides. Generally, the binding constants increase with increasing π-electron density on the guest (Table 5). However, there are some anomalies (*e.g.* with

Table 5 Association constants for receptor **36** with benzoic acid derivatives in chloroform at 298 K

Guest	K/M^{-1}
3-Ethoxycarbonylbenzoic acid	1.47×10^3
2-Toluic acid	3.52×10^4
Benzoic acid	6.00×10^4
4-Ethoxybenzoic acid	1.53×10^5
3,4-Methylenedioxybenzoic acid	1.58×10^5
3,4,5-Trimethoxybenzoic acid	2.41×10^4
3-Dimethylaminobenzoic acid	8.21×10^5
4-Dimethylaminobenzoic acid	1.56×10^6

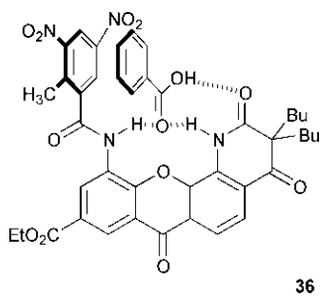

36

Fig. 25 Crego's clefts bind benzoic acid derivatives.

3,4-methylenedioxybenzoic acid) indicating that the system is more complicated.

Moore and co-workers prepared hexakis(phenylacetylene) molecules (PAMs) with varying degrees of electron withdrawing (ester) and donating (alkyl ether) substituents and studied their aggregation properties by ^{1}H NMR in chloroform (Fig. 26(a)).[62,63] The chemical shifts of the aromatic protons depend strongly on concentration, and dimerisation through aromatic stacking interactions was proposed to account for this. Compounds **37**, **38** and **39** show dimerisation constants of 60, 18 and 26 M^{-1} respectively. Compounds **40** and **41** show no aggregation behaviour. These results indicate that the aromatic substituents have a significant influence on the stacking interaction. *tert*-Butyl ester substituents prevent aggregation, indicating that the interaction is due to face-to-face stacking which is hindered by the bulky groups. Non-planar pentakis- and heptakis-(phenylacetylene) molecules also have reduced association constants. Tobe *et al.* designed a PAM system capable of heteroaggregation and binding metal ions (Fig. 26(b)).[64] Compounds **42** and **43** form a 1 : 1 heteroaggregate but **42** does not self-associate. The electron withdrawing cyano-substituents appear to enhance aromatic stacking interactions in the heteroaggregate.

6.2 Intramolecular interactions

Moore and co-workers designed oligomers based on the PAMs [65] and showed that these phenylacetylene oligomers fold up in a process driven by solvation (Fig. 26(c)). Hypochromic effects measured in several solvents were used as a measure of conformational changes. When $n = 8$ in acetonitrile, the oligomers formed an ordered structure consistent with a helix. ^{1}H NMR studies in chloroform showed negligible changes in chemical shift with increasing chain length, whereas in acetonitrile, upfield shifts were observed for the phenyl protons, and these increased dramatically as n increased from 8 to 14. The helical structure minimises interactions of the hydrocarbon backbone with the solvent and maximises intramolecular aromatic stacking.

Iverson *et al.* have also used aromatic stacking interactions to dictate the secondary structure of synthetic oligomers in solution.[66] The system consists of electron acceptor (naphthalene-1,8 : 4,5-tetracarboxylic diimide) and electron donor (1,5-dialkoxynaphthalene) units, selected because the monomers are known to form a stable complex in water ($K = 130$ M^{-1}).

(a)

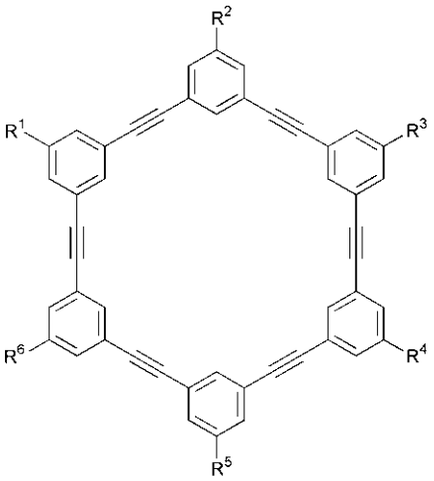

37 $R^{1\text{-}6} = CO_2n\text{-Bu}$
38 $R^{1,3,5} = CO_2n\text{-Bu}$, $R^{2,4,6} = On\text{-Bu}$
39 $R^{1,2,3} = CO_2n\text{-Bu}$, $R^{4,5,6} = On\text{-Bu}$
40 $R^{1\text{-}6} = On\text{-Bu}$
41 $R^{1\text{-}6} = CH_2On\text{-Bu}$

(b)

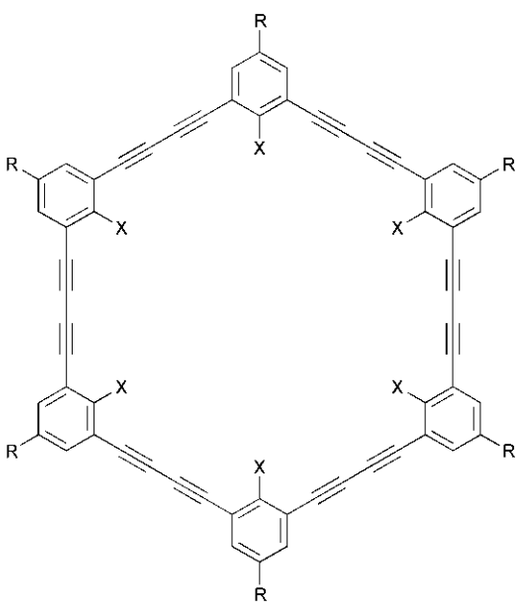

42 R = $CO_2C_8H_{17}$, X = CN
43 R = $CO_2C_8H_{17}$, X = H

(c)

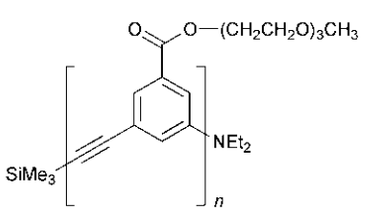

n = 2,4,6,8,10,12,14,16,18

Fig. 26 (a) Moore's macrocyclic phenylacetylene molecules (PAMs). (b) Tobe's macrocyclic PAMs. (c) Moore's open chain PAMs which fold in acetonitrile.

A co-crystal of the two monomers showed the electron donors and acceptors in an alternating stack (Fig. 27). Molecular mechanics together with the X-ray crystal structure were used to determine an ideal backbone length to allow the electron donor and acceptor units to be linked in a chain but still form a stacked arrangement in solution: L-aspartic acid residues were used. The "aedemers" in Fig. 28 were prepared by solid

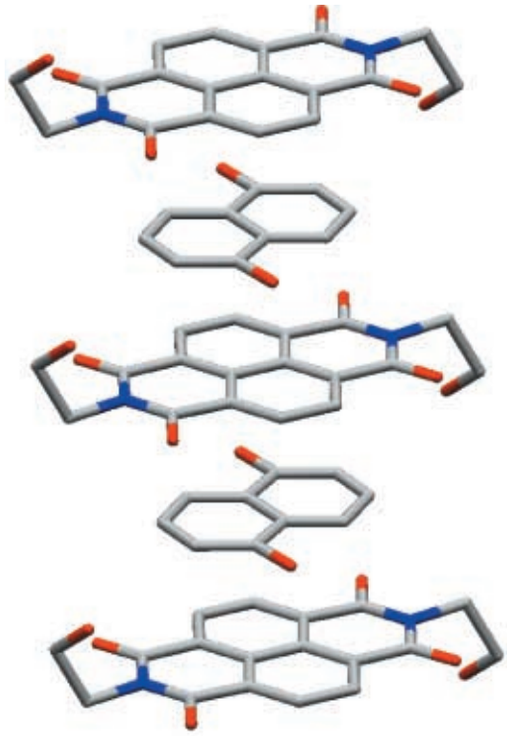

Fig. 27 Structure of the co-crystal of a 1,4,5,8-naphthalenetetracarboxylic diimide and a 1,5-dialkoxynapthalene.

phase synthesis. Spectroscopic evidence for $n = 2$ and 3 is consistent with a pleated structure where the aromatic rings are all stacked as shown.

The electron acceptor unit was also used in the synthesis of a tetraintercalator connected by four tetrapeptide linkers (Fig. 29).[67] One lysine residue was placed on each segment to provide electrostatic attraction to DNA. Hypochroism, unwinding studies, kinetics, DNAase and chemical footprinting show that the polyintercalators have a preference for GC sequences, and a cooperative mode of binding was proposed.

As we have already seen, the hydrophobic effect has a significant influence on aromatic interactions, water preferring to interact with itself rather than with aromatic surfaces. Newcomb and Gellman carried out a series of experiments to investigate this effect for two covalently tethered aromatic groups. A comparison of the stacking tendencies of hydrocarbon (phenyl and naphthyl) and heterocycle (adenine) rings in aqueous solution was carried out using ^{1}H NMR spectroscopy to study the conformational properties of carboxylate derivatives **44**–**48** (Fig. 30).[68] Large negative shifts of the adenine protons of **44** were observed compared with the control **47**. This is indicative of an intramolecular aromatic interaction in **44**. In contrast, **45** and **48** have similar spectra which indicates that there is no intramolecular interaction for the dinaphthyl derivative. An X-ray structure of a phenyl derivative **49** showed the phenyl rings splayed far apart. In **46**, negative shifts on both rings indicate significant stacking. DMSO destroyed the interaction. If the intramolecular stacking were due solely to the hydrophobic effect, then **45** would exhibit a stacking interaction. The results are most consistent with the alignment of partial positive and negative charges on neighbouring groups as the main force influencing the stacking interactions.

Naphthyl units connected by a flexible linker were prepared to further probe hydrophobic collapse.[69] The three atom linker previously used forced a near parallel arrangement, but the four atom linker in **50** allowed different approaches of the aromatic moieties. An X-ray crystal structure of **50** showed an edge-to-face arrangement of the naphthyl rings, and ^{1}H NMR experiments showed that the naphthyl rings are in close proximity in

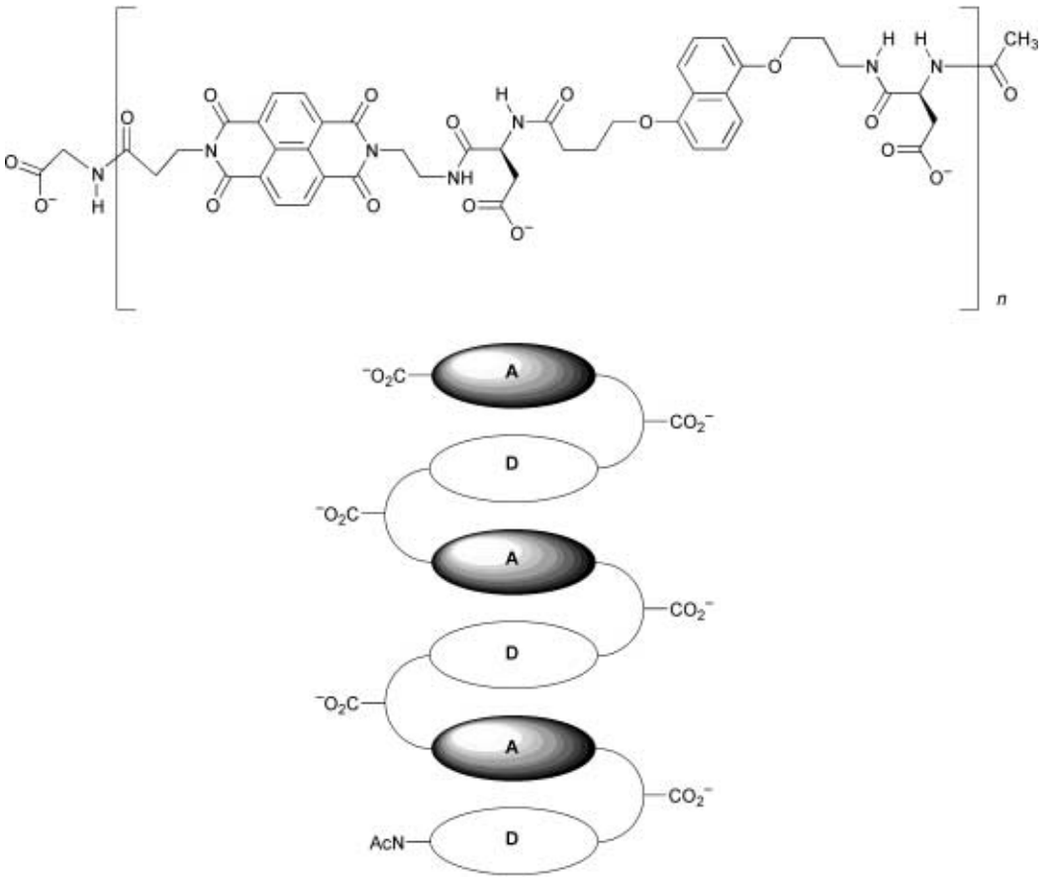

Fig. 28 Structure of Iverson's aedemers (n = 1, 2, 3) and a cartoon of the folded solution structure.

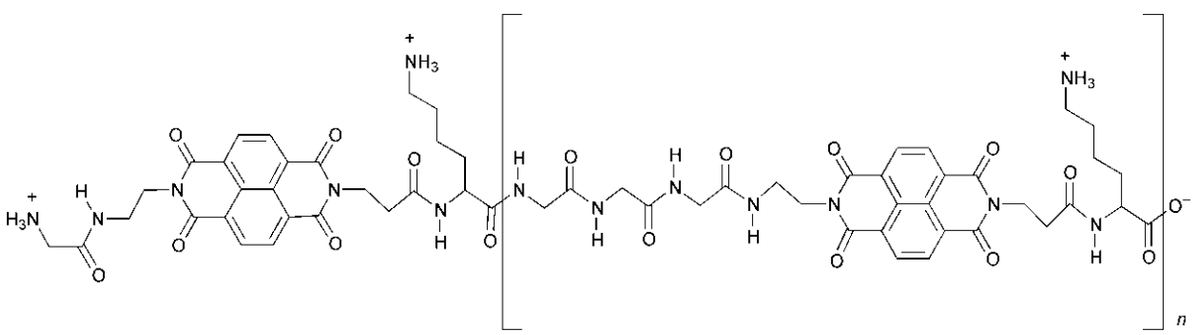

Fig. 29 Polyintercalators based on diimide amino acid oligomers (n = 1, 2, 3, 4).

aqueous solution. The chemical shift differences between **50** and **51** in benzene were very similar to those in water which suggests that the hydrophobic effect has little influence on the folding of this molecule.

Kollman and co-workers recently used a combination of modelling and NMR studies on similar compounds with different results.[70] The possible geometries of the indole derivative **52** were calculated theoretically. The linker allows the molecule to adopt edge-to-face, offset stacked, face-to-face stacked and non-stacked conformations. The calculations suggested that the edge-to-face and non-stacked conformations are the most stable in water. ^{1}H NMR studies on **52** showed a larger population of the edge-to-face stacked conformation in water than in DMSO at 22 °C.

Jimenez-Barbero used a similar approach to investigate stacking interactions in benzene using ester linked aromatic units **53**–**58** (Fig. 31).[71] The ^{1}H NMR spectrum of the symmetrical diesters **54** and **56** and corresponding control monoesters **53** and **55** are very similar, indicating there is no intramolecular interaction. However, the spectrum of the unsymmetrical diester **57** shows upfield shifts of between 0.1 and 0.5 ppm on both the anthracene and dinitrophenyl rings. A stacked intramolecular complex was proposed. If van der Waals interactions were dominant in the complex, the greatest effect would be in the symmetrical anthracene derivative, as it would provide the largest van der Waals contact. No charge-transfer bands in the UV spectra were observed. Hence the interaction was attributed to electrostatic quadrupole interactions, as the quadrupole moments of the dinitrophenyl and anthracene groups have opposite signs.

Breault *et al.* used metal tris(bipyridine) complexes **59** and **60** to investigate the influence of solvent on aromatic interactions.[72] The differences between the chemical shifts of the bipyridine protons in the presence of pendant alkyl and aromatic esters were used to quantify the aromatic interaction as a function of solvent (Fig. 32). Large upfield shifts were observed in polar solvents such as water, and the magnitude of the shift decreased as the solvent polarity decreased. This is consistent with the solvophobic description of aromatic interactions as seen in the Diederich cyclophane system.[73] However, as the solvent polarity was decreased further, the strength of the aromatic interaction went through a minimum in DMSO and

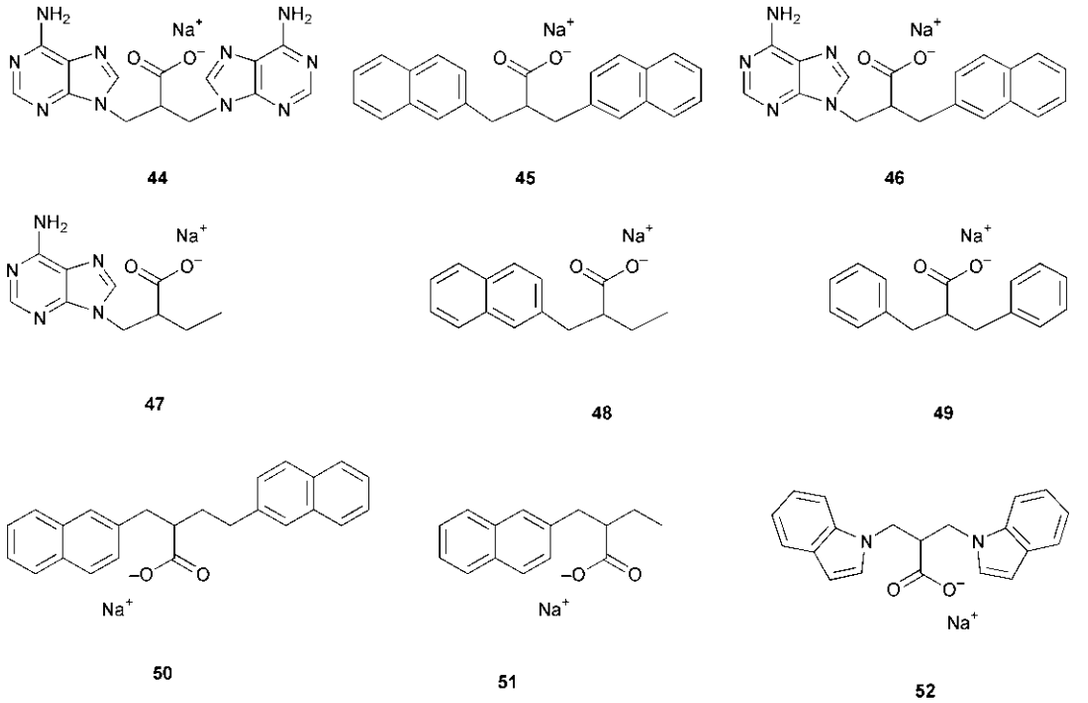

Fig. 30 Compounds used to probe intramolecular aromatic interactions in water.

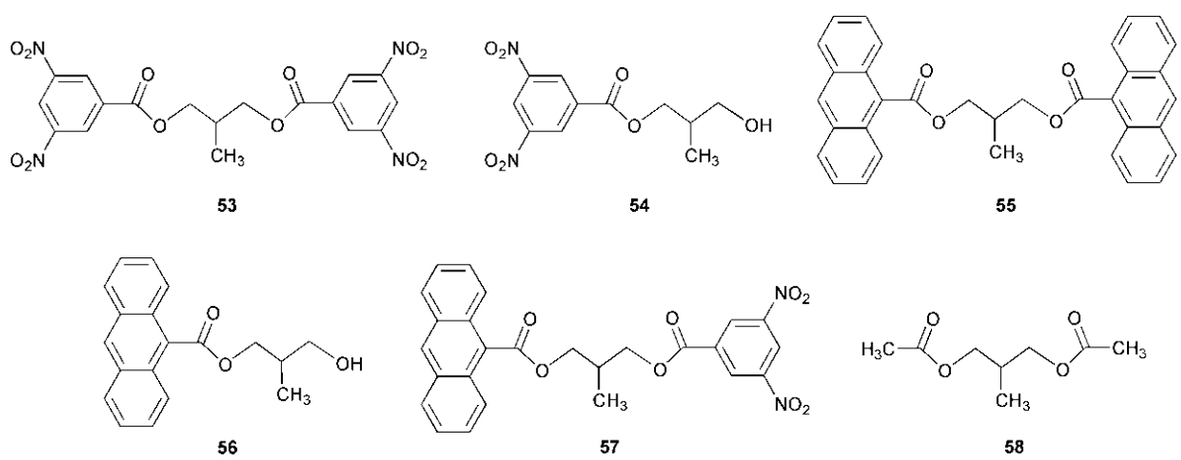

Fig. 31 Compounds used to probe intramolecular aromatic interactions in benzene.

then started to increase again, and in chloroform the interaction is comparable to that in water. These results suggest that in non-polar solvents, electrostatic interactions become dominant and lead to significant attractive interactions between the aromatic rings.

Stoddart and co-workers have used aromatic stacking interactions to direct the synthesis and influence the properties of a large number of catenanes, pseudorotaxanes and rotaxanes. Initially a 1 : 1 complex was observed between di-*p*-phenylene-34-crown-10 and paraquat dication (Fig. 33(a)).[74] The complex between a tetracationic ring based on paraquat and 1,4-dimethoxybenzene was also crystallised (Fig. 33(b)), and this revealed the aromatic stacking interactions that are responsible for complexation. The interactions in these complexes formed the basis of the template directed synthesis of a [2]catenane (Fig. 33(c)).[75] This initial design led to higher order catenanes, the largest being a [7]catenane which was synthesised under high pressure.[76] Pseudorotaxanes followed and stoppering the ends of the thread of the pseudorotaxane resulted in [2]rotaxanes. Again, higher order pseudorotaxanes and rotaxanes were synthesised and characterised.[77] A summary of the approach to pseudorotaxanes, rotaxanes and catenanes is shown in Fig. 34.[78]

Table 6 Barriers to rotation for substituted 1,8-diarylnaphthalene molecules

Substituent	$\Delta G^{\ddagger}$/kJ mol^{-1}
OMe	58.2
Me	60.2
H	61.5
Cl	64.9
CO_2Me	70.7
NO_2	72.4

7 Quantitative approaches to aromatic interactions

Cozzi and Siegel and co-workers used substituted 1,8-diarylnaphthalene molecules to measure the barrier to rotation of the phenyl rings in chloroform using dynamic NMR (Fig. 35(a)), and the results are shown in Table 6.[79] The activation energy for the isomerism provides a measure of the strength of the aromatic interaction between the stacked phenyl rings in the ground state. These results were plotted against Hammett substituent constants, and a linear relationship was found which indicates that electrostatic effects are the most important factor in this system. There was no UV–visible spectroscopic evidence

for a charge-transfer interaction between the phenyl rings. The experimental evidence that the barrier increases on passing from an electron donating group to an electron withdrawing group as substituent led to the conclusion that a significant polar π-interaction exists between the phenyl rings.[80] When

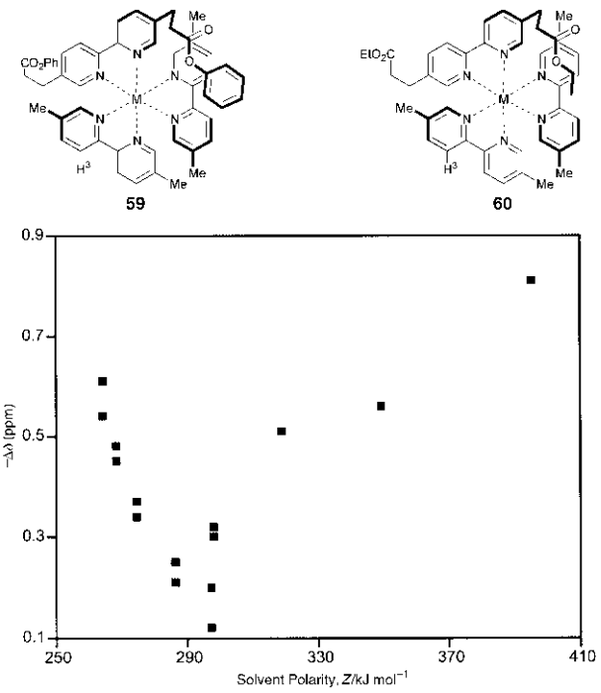

Fig. 32 Metal complexes for studying solvent effects on aromatic interactions. $\Delta\delta = \delta(H_3 \text{ in } \mathbf{59}) - \delta(H_3 \text{ in } \mathbf{60})$.

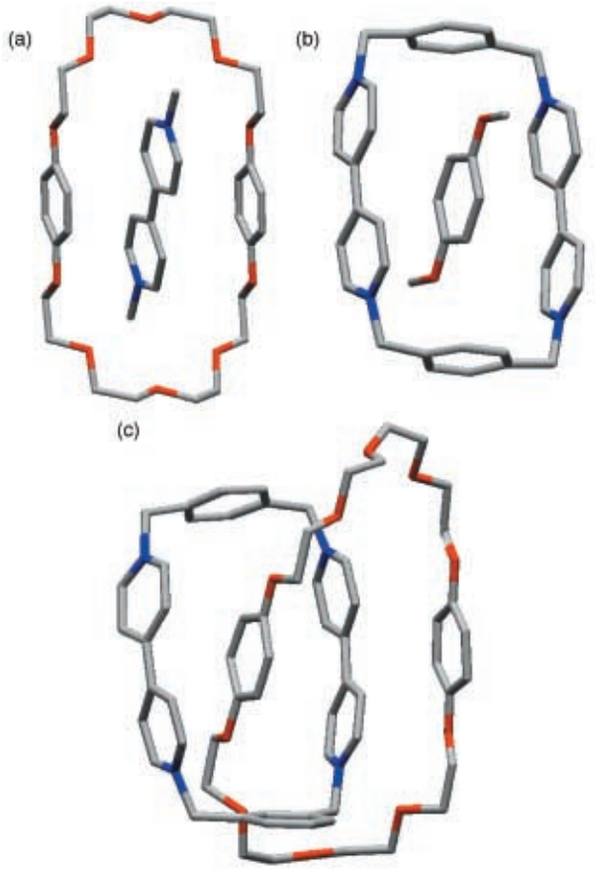

Fig. 33 Host–guest complexes formed by the Stoddart macrocycles (a) and (b), and the corresponding [2]catenane (c).

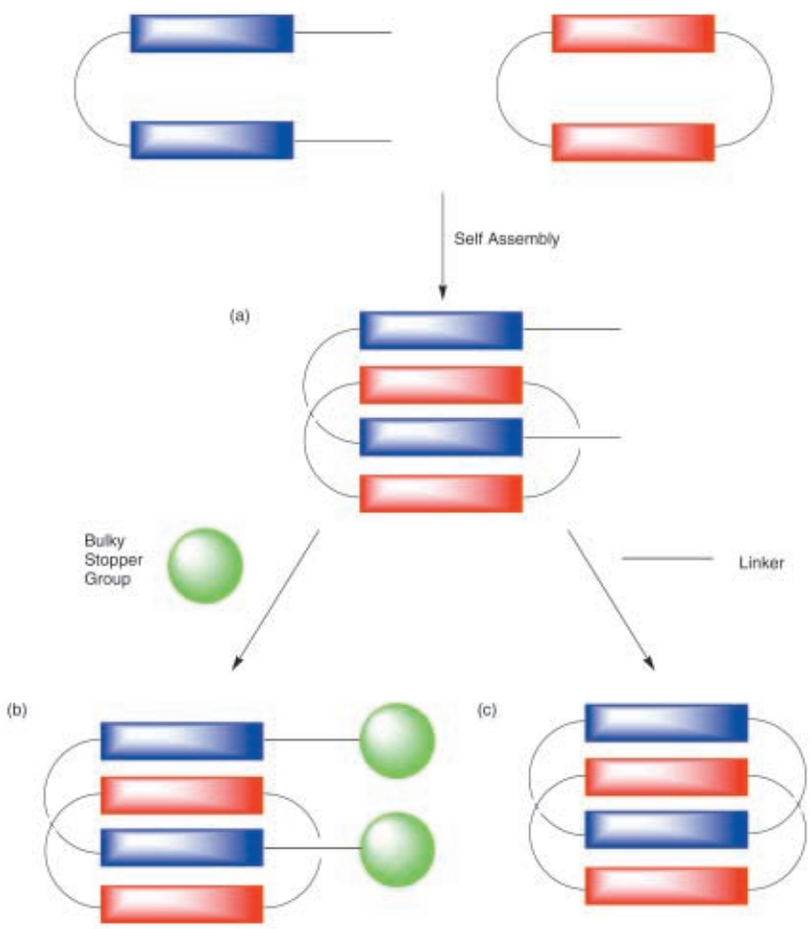

Fig. 34 Synthetic approaches to rotaxanes (b) and catenanes (c) using aromatic stacking interactions to organise the key pseudorotaxane intermediate (a).

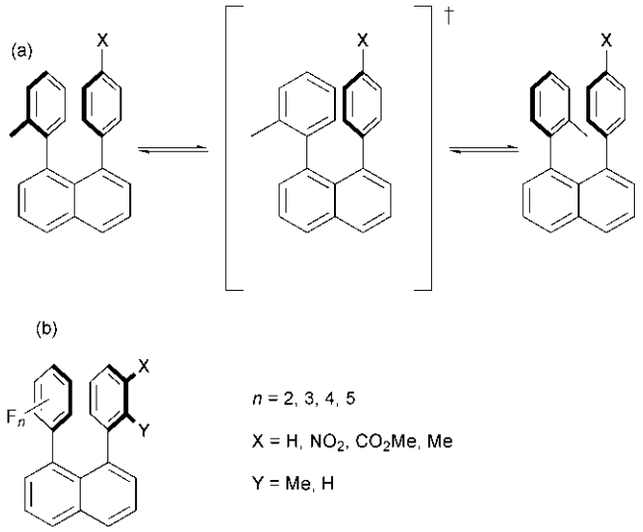

Fig. 35 (a) Dynamic equilibrium used to quantify substituent effects on aromatic stacking interactions between substituted phenyl rings (X = OMe, Me, H, Cl, CO_2Me, NO_2). (b) Fluorination of the 1,8-diarylnaphthalene derivatives changes the quadrupole moment of the aromatic ring and consequently the trends in stacking interaction energy.

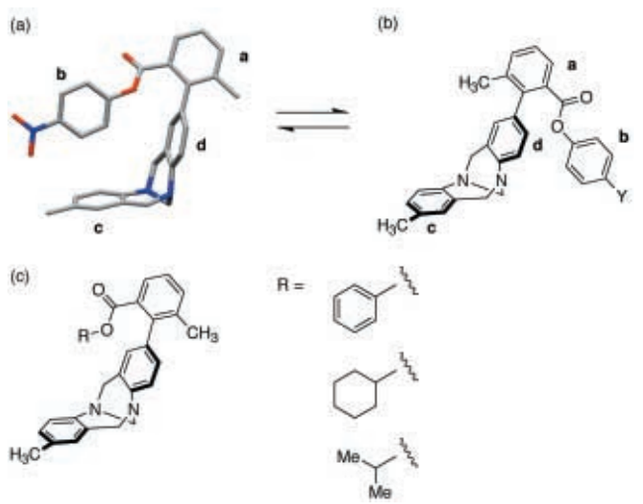

Fig. 36 Wilcox's torsion balance used to quantify the interaction between rings **b** and **c**. The X-ray structure of the folded conformation is shown (a). The approach was used to measure interactions of a range of functional groups with the face of an aromatic ring (c).

substituents were present on both aromatic rings, a linear relationship was obtained between the barrier to rotation and the sum of the Hammett substituent constants. If a CT interaction were dominant then the donor–acceptor interaction would be most favourable, followed by the acceptor–acceptor and finally the donor–donor interaction. The experimental results show that this is not true: the most favourable interaction is acceptor–acceptor followed by donor–acceptor and finally donor–donor interactions. The most reasonable explanation for such a trend is that the electron withdrawing groups decrease the repulsive interactions between the π-electron density of the phenyl rings, when they are in a forced stacked conformation.

A test for the electrostatic model was to reverse the charge distribution in the quadrupole of the aromatic rings. Several fluorinated compounds were investigated for this purpose (Fig. 35(b)).[81] Progressive fluorination of one phenyl ring increased the barrier to rotation, due to a decrease in the mutual repulsion by removal of electron density from the π-systems by the electronegative fluorines. The perfluorinated ring with a reversed quadrupole moment reversed the trend in

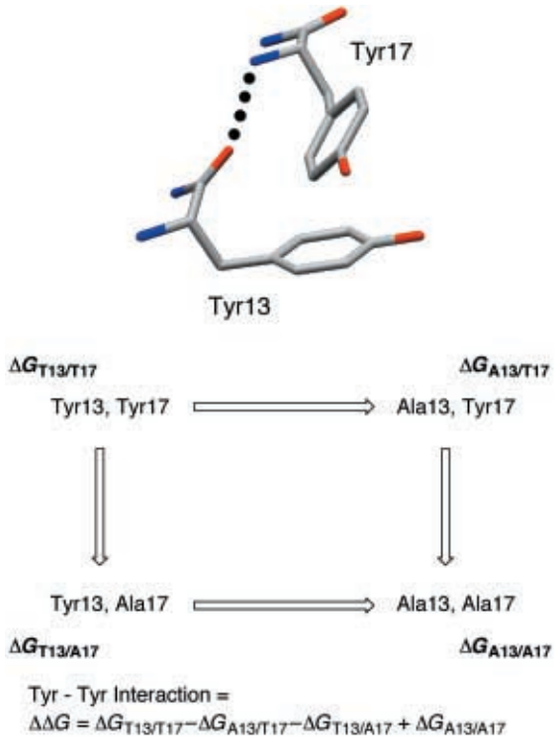

Fig. 37 The double mutant cycle used to quantify the tyrosine–tyrosine interaction in barnase. The geometry of interaction in the X-ray crystal structure of the wild type protein is shown.

the barriers to rotation as a function of substitution of X. These results suggest that it is electrostatics that govern the magnitude of the stacking interaction in this system.

Wilcox and co-workers constructed a molecular balance capable of measuring edge-to-face aromatic interactions using conformational isomerism as shown in Fig. 36.[82] In the folded conformation, the edge of ring **b** lies over the face of ring **c** (Fig. 36(a)). In the open conformation, rings **b** and **c** are remote (Fig. 36(c)). While both conformations include an interaction between rings **b** and **d**, this does not perturb the relative populations. The two conformations interconvert by slow rotation at room temperature. Deviations from a 1 : 1 ratio of states provide a measure of the **b**–**c** interaction. When Y = H the folded state is preferred, substitution with a methyl group shifts the equilibrium slightly, but a methoxy group has no effect. When Y = I, CN or NO_2, there is an enhanced preference for the folded state which suggests that electrostatic effects are important in the edge-to-face interaction. However, phenyl, cyclohexyl and isopropyl groups all show similar affinities for the face of the aryl ring **c**.[83] A range of electron donating and withdrawing groups were used (X = NH_2, OH, CH_3, I, Br, CN, and NO_2). The folding energies of the isopropyl and phenyl esters were found to be -2.0 ± 0.4 and -1.3 ± 0.4 kJ mol^{-1} respectively for all X substituents. This result suggests that electrostatic forces are not important and that London dispersion forces are more important in governing the edge-to-face interaction. However, these systems are not fully understood as the populations of the two states are unaffected by changes in solvent.

Following the observations by Burley and Petsko[40] concerning the frequency of aromatic interactions in proteins, Fersht *et al.* measured the magnitude of such an interaction using a double mutant cycle.[84] An aromatic pair on the first α-helix of barnase was the interaction of interest. The edge of the aromatic ring of Tyrosine 17 (Tyr17) interacts with the face of the aromatic ring in Tyrosine 13 (Tyr13) (Fig. 37). In order to determine the strength of the interaction, it was necessary to remove it by mutating one of the residues involved, and then

Table 7 Edge-to-face aromatic interactions (kJ mol^{-1}) in zipper complexes measured in $CDCl_3$ at 295 K

	Substituent X		
Substituent Y	NO_2	H	NMe_2
NO_2	+1.2	−0.2	−1.4
H	−3.4	−1.4	−1.1
NMe_2	−4.6	−1.8	−0.9

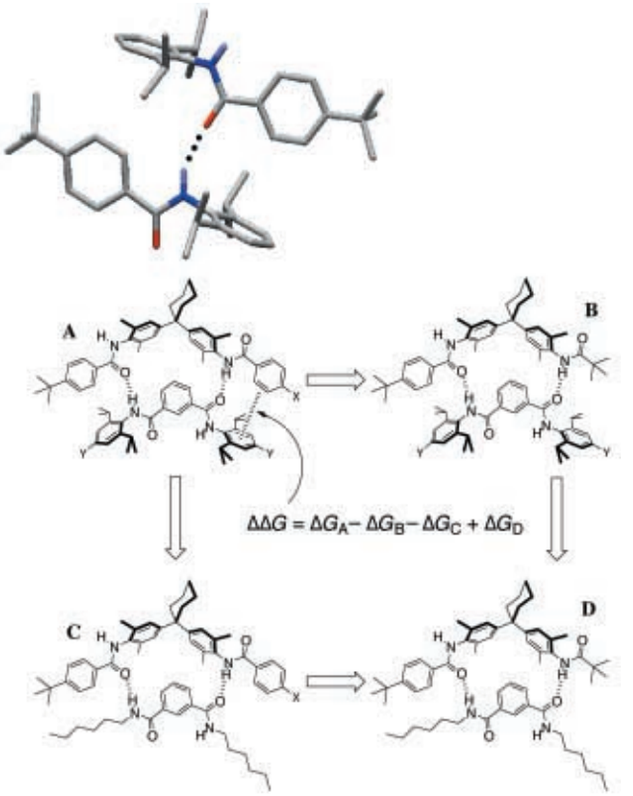

Fig. 38 Chemical double mutant cycle to measure the terminal edge-to-face aromatic interaction in complex A. The inset shows the X-ray crystal structure of a model compound which contains the same intermolecular interaction.

measure the difference in stability between the mutated protein and wild type. This is useful when the amino acids make no other contacts in the protein, but this is generally not true, and the analysis of a single mutant is therefore misleading. A double mutant cycle allows the isolation of the energetics of pairwise interactions between two residues in a protein even when they take part in multiple interactions. The two residues involved in the interaction are replaced by alanine initially as single mutations, and then as a double mutation (Fig. 37). In the first instance, Tyr13 was replaced by alanine (Ala13). The change in free energy of unfolding was measured by denaturation using urea. The measurement was then repeated on the mutation of Tyr17 to alanine (Ala17). These mutations each measure the edge-to-face interaction of interest as well as secondary interactions with the surrounding residues. In order to quantify these secondary interactions, the double mutant Ala13, Ala17 is used. Any effects of mutations that do not involve the interaction between the two residues of interest cancel out in the thermodynamic analysis in Fig. 37. The free energy for the edge-to-face interaction between Tyr13 and Tyr17 was found to be -5.6 ± 0.3 kJ mol^{-1}. The authors conclude that an aromatic pair in the hydrophobic core of a protein can make a large contribution to the stability of a protein.

Hunter *et al.* used a similar approach to measure edge-to-face interactions in a synthetic system. H-bonded molecular zippers

Fig. 39 The X-ray crystal structure of d(CGCGAAAAAACG) (blue) with the calculated structure overlaid in red. Only the aromatic bases are shown for clarity.

were used to construct a chemical double mutant cycle (Fig. 38).[85] The association constants of all four complexes were determined by ^{1}H NMR titration and the edge-to-face interaction for unfunctionalised aromatic rings (X = Y = H) was found to be -1.4 ± 0.8 kJ mol^{-1} in chloroform. An X-ray crystal structure of a model compound was used to probe the geometry of the interaction at the terminus of the zipper and confirmed an edge-to-face arrangement of aromatic rings (Fig. 38). Substituent effects were investigated by substituting the edge and face rings with electron withdrawing and electron donating groups (Table 7).[86] These values correlate with Hammett substituent parameters for X and Y (σ), shown in eqn. (2). The last three terms in the equation were interpreted as

$$\Delta\Delta G\,(\pi\text{–}\pi) = 5.2\,\sigma_X\sigma_Y - 1.9\,\sigma_X + 1.4\,\sigma_Y - 1.5 \quad (2)$$

an electrostatic interaction between the positively charged CH groups on the edge ring and the negatively charged π-electron density on the face ring. The first term is attractive when X and Y have opposite effects which reflects an electrostatic interaction between the overall dipoles caused by the polarising effects of the substituents.

8 Applications of aromatic interactions

The knowledge gained from studies of aromatic interactions is slowly increasing and the results obtained are being used to understand and rationally design new functional molecular systems. In order to understand the complex recognition

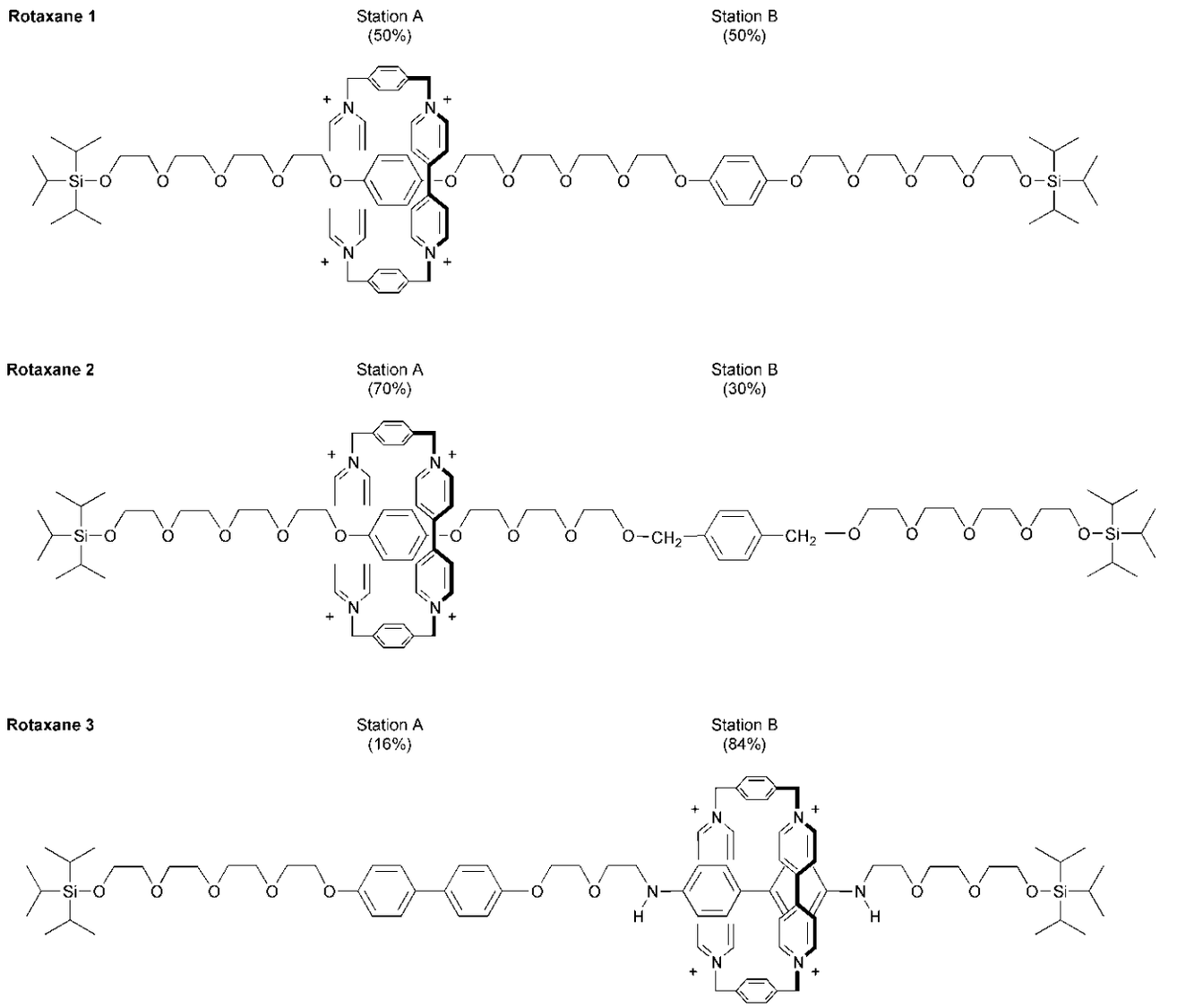

Fig. 40 Unsymmetrical rotaxanes and populations at each station.

processes that are associated with DNA, proteins and other biological systems, it is important that we understand the underlying mechanisms. As aromatic moieties are abundant in these biological structures, an understanding of the fundamental interactions between them is vital to further study more complex systems.

Hunter *et al.* have modelled DNA base stacking interactions, and the results correlate well with oligonucleotide X-ray crystal structures.[87] This approach has been used to parametrise a complete model for predicting the sequence-dependent structure of DNA. Structures calculated for dodecamers agree with X-ray crystal structures to within 1 Å rms difference in the positions of the heavy atoms (Fig. 39). The results explain the origins of some fundamentally important properties. For example, the TATA sequence is the origin of replication, because this is the least stable of all DNA tetranucleotides and so is relatively easy to open. There are three reasons: TA base pairs have two H-bonds rather than the three found in GC base pairs; the stacking interactions are weaker than for any other dinucleotide, and the conformational properties of TA and AT steps are incompatible which puts strain on the backbone. Thus theoretical models of aromatic stacking interactions are beginning to contribute to our understanding of complex biological processes.[88,89]

Stoddart and co-workers have used aromatic stacking interactions to control the behaviour of a molecular shuttle. A symmetrical rotaxane with multiple donor "stations" on the thread exhibits a translational equilibrium, with the tetracationic ring rapidly interchanging between the two stations.[90] However if the thread is unsymmetrical, then the ring exhibits an affinity for one station over another, due to differences in the aromatic interactions (Fig. 40). In rotaxane 1, the ring spends 50% of its time on each station, with a barrier to shuttling of 54 kJ mol^{-1}. In rotaxane 2, the ring spends 70% of its time on station A, because of a stronger stacking interaction with the dialkoxyphenyl ring. In rotaxane 3, the ring prefers to interact with the benzidine station. Rotaxane 3 can be switched between the two conformations chemically or electrochemically.[91] Protonation of the benzidine station with TFA causes electrostatic repulsion with the tetracationic ring which moves onto station A. Addition of pyridine reverses this process. Electrochemical oxidation of the benzidine group leads to charge–charge repulsion and again causes the tetracationic ring to sit over the biphenol station.

Stacking interactions play a key role in determining the material properties of molecular solids. Perhaps the best studied cases are the semi-conducting charge-transfer complexes based on tetrathiofulvalene and tetracyanoquinone derivatives.[92] Semi-conducting properties are obtained provided the molecules can be persuaded to form segregated stacks. Although there has been little success in engineering the crystal packing of such molecules, this is clearly an area of great potential where controlling the aromatic stacking interactions would lead to control over functional properties.

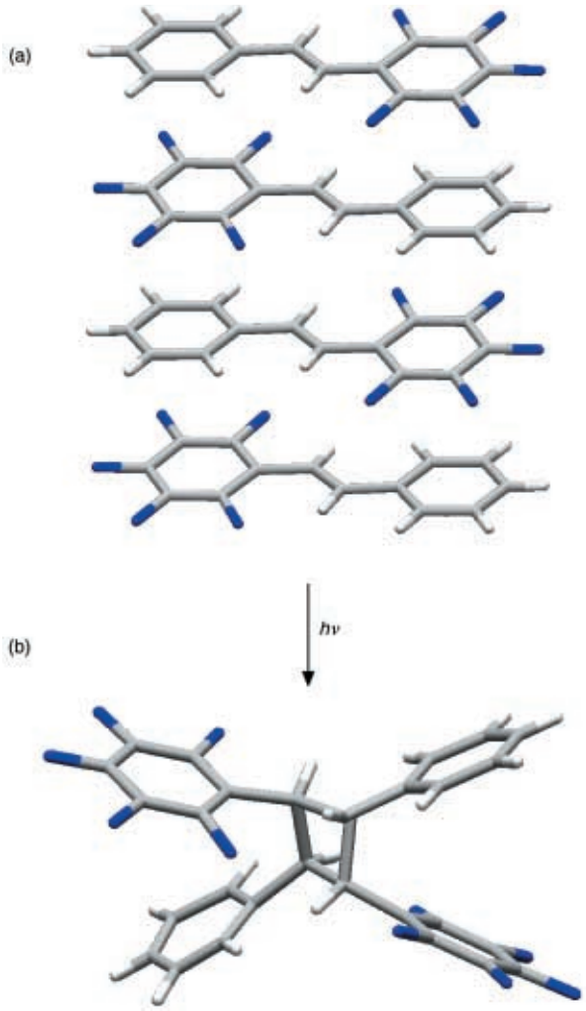

Fig. 41 Phenyl–pentafluorophenyl stacking interactions control the packing of a stilbene derivative in the solid state (a) and hence the stereochemistry of the cyclobutane photodimer (b).

Coates *et al.* used stacking interactions in the solid state to influence the photodimerisation of olefins. In a similar manner to the way that benzene and hexafluorobenzene form face-to-face stacks, (*E*)-pentafluorostilbene crystallises with long stacks of alternating phenyl and pentafluorophenyl rings (Fig. 41(a)), and this leads to a single isomer of the cyclobutane photodimer (Fig. 41(b)). Dougherty used stacking interactions in the solid state to align monomeric units for polymerisation.[93] A diyne normally polymerises to give a (*E*)-polybutadiyne as shown in Fig. 42(a). If a stacked arrangement of butadiyne units could be obtained, this should lead to (*Z*)-polymerisation (Fig. 42(b)). Diphenylbutadiyne and decafluorodiphenylbutadiyne were co-crystallised, and the crystal structure revealed the acetylenes packed alternately in well ordered phenyl·pentafluorophenyl stacks. The mixed phenyl–pentafluorophenyl diyne compound also crystallises with phenyl·pentafluorophenyl stacks, so that the molecules sit in a head-to-tail arrangement which appears ideal for (*Z*)-polymerisation (Fig. 43). However, no structural data on the products of polymerisation reactions have been published.

Important aromatic interactions have been found in synthetic catalytic systems. Sharpless *et al.* used the ligand in Fig. 44 in combination with osmium tetraoxide to influence transition states in osmium-catalysed asymmetric dihydroxylation reactions.[94] The ligand adopts a U-shaped geometry with the naphthyl groups forming a tweezer-like binding pocket which sandwiches aromatic substituents on olefins and holds the double bond in the perfect position to react with the osmium tetraoxide. Aromatic substrates react faster than aliphatic ones,

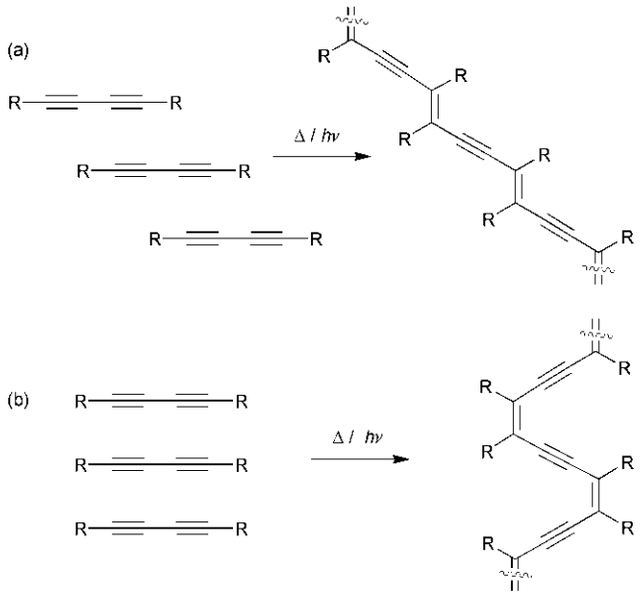

Fig. 42 (a) Formation of (*E*)-polybutadiene. (b) Arrangement of monomers required to yield the (*Z*) polymer.

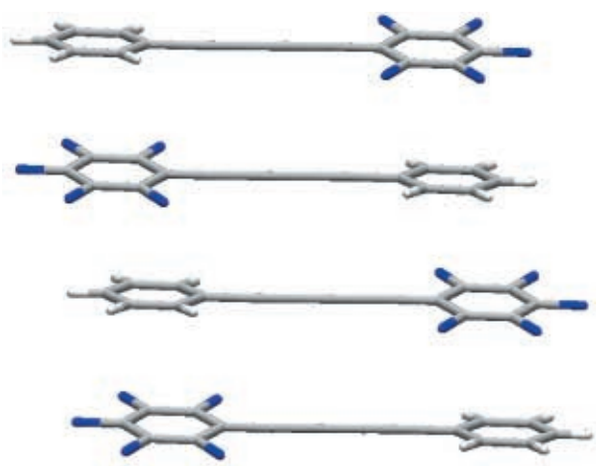

Fig. 43 X-Ray crystal structure of 1-(2,3,4,5,6-pentafluorophenyl)-4-phenylbutadiyne.

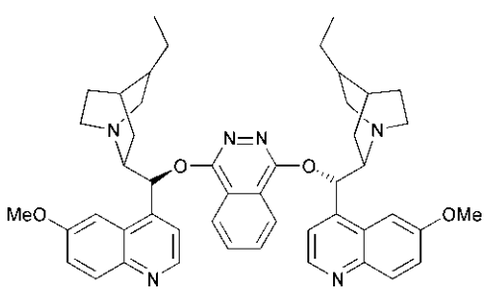

Fig. 44 The Sharpless ligand used for the asymmetric dihydroxylation of olefins.

and increasing the size of the aromatic group in both ligand and substrate leads to larger rate constants due to favourable stacking interactions in the binding pocket.

9 Conclusions

The picture that emerges is that aromatic interactions are not so different from simple interactions like H-bonds: they are just complicated by the fact that larger functional groups are involved. The major difference is that the surface area of intermolecular contact is large, so van der Waals interactions and desolvation are much more important. Although the

electrostatic principles governing the magnitudes of H-bonds also apply to aromatic interactions, there are many more contact points where electrostatic interactions have to be considered, and so it is difficult to rationalise the behaviour of aromatic interactions with straightforward rules as in the case of H-bonds. Nevertheless, our understanding has progressed to the stage where we can produce useful computer models which describe the properties of aromatic interactions well, and a range of robust aromatic interaction motifs have been developed for use in the rational design of new molecular functions.

10 References

1 R. S. Mulliken, *J. Am. Chem. Soc.*, 1950, **72**, 600.
2 L. J. Andrews, *Chem. Rev.*, 1954, **54**, 713.
3 J. Landauer and H. McConnell, *J. Am. Chem. Soc.*, 1952, **74**, 1221.
4 M. G. Lawrey and H. McConnell, *J. Am. Chem. Soc.*, 1952, **74**, 6175.
5 C. A. Hunter and J. K. M. Sanders, *J. Am. Chem. Soc.*, 1990, **112**, 5525.
6 D. B. Chesnut and R. W. Moseley, *Theor. Chim. Acta*, 1969, **13**, 230.
7 M. J. Mantoine, *Theor. Chim. Acta*, 1969, **15**, 141.
8 P. Linse, *J. Am. Chem. Soc.*, 1992, **114**, 4366.
9 W. L. Jorgensen and D. L. Severance, *J. Am. Chem. Soc.*, 1990, **112**, 4768.
10 R. L. Jaffe and G. D. Smith, *J. Chem. Phys.*, 1996, **105**, 2780.
11 C. Chipot, R. Jaffe, B. Maigret, D. A. Pearlman and P. A. Kollman, *J. Am. Chem. Soc.*, 1996, **118**, 11217.
12 P. Carsky, H. L. Selzle and E. W. Schlag, *Chem. Phys.*, 1988, **125**, 165.
13 P. Hobza, H. L. Selzle and E. W. Schlag, *J. Chem. Phys.*, 1990, **98**, 5893.
14 P. Hobza, H. L. Selzle and E. W. Schlag, *J. Phys. Chem.*, 1993, **97**, 3937.
15 R. L. Jaffe and G. D. Smith, *J. Phys. Chem.*, 1996, **100**, 9624.
16 K. C. Janda, J. C. Hemminger, S. E. Novick, S. E. Harra and W. Klemperer, *J. Chem. Phys.*, 1975, **63**, 1419.
17 J. M. Steed, T. A. Dixon and W. Klemperer, *J. Chem. Phys.*, 1979, **70**, 4940.
18 P. R. R. Langridge-Smith, D. V. Brumbaugh, C. A. Haynam and D. H. Levy, *J. Phys. Chem.*, 1981, **85**, 3742.
19 D. H. Levy, C. A. Haynam and D. V. Brumbaugh, *Faraday Discuss. Chem. Soc.*, 1982, **73**, 137.
20 S. L. Price and A. J. Stone, *J. Chem. Phys.*, 1987, **86**, 2859.
21 M. M. Doxtader, E. A. Mangle, A. K. Bhattacharya, S. M. Cohen and M. R. Topp, *Chem. Phys.*, 1986, **101**, 413.
22 L. Young, C. A. Haynam and D. H. Levy, *J. Chem. Phys.*, 1983, **79**, 1592.
23 C. R. Patrick and G. S. Prosser, *Nature*, 1960, 1021.
24 T. Dahl, *Acta Chem. Scan. Ser. A*, 1975, **29**, 170.
25 A. Gavezzotti, *Chem. Phys. Lett.*, 1989, **161**, 67.
26 A. Gavezzotti and G. R. Desiraju, *Acta Crystallogr., Sect. B*, 1988, **44**, 427.
27 G. R. Desiraju and A. Gavezzotti, *Acta Crystallogr., Sect. B*, 1989, **45**, 473.
28 G. R. Desiraju and A. Gavezzotti, *J. Chem. Soc., Chem. Commun.*, 1989, 621.
29 J. D. Watson and F. H. Crick, *Nature*, 1953, **171**, 737.
30 W. Saenger, *Principles of Nucleic Acid Structure*, Springer-Verlag, New York, 1988.
31 B. H. Zimm, *J. Chem. Phys.*, 1960, **33**, 1349.
32 D. M. Crothers and B. H. Zimm, *J. Mol. Biol.*, 1967, **9**, 1.
33 S. I. Chan, M. P. Schweizer, P. O. P. Ts'O and G. K. Helmklamp, *J. Am. Chem. Soc.*, 1964, **86**, 4183.
34 M. P. Schweizer, S. I. Chan and P. O. P. Ts'O, *J. Am. Chem. Soc.*, 1965, **87**, 5241.
35 K. Mutai, B. A. Gruber and N. J. Leanord, *J. Am. Chem. Soc.*, 1975, **97**, 4095.
36 S. M. Freier, K. O. Hill, T. G. Dewey, L. A. Marky, K. J. Breslauer and D. H. Turner, *Biochem.*, 1981, **20**, 1419.
37 F. Martin, O. C. Uhlenbeck and P. Doty, *J. Mol. Biol.*, 1971, **57**, 201.
38 K. M. Guckian, B. A. Schweitzer, R. X. F. Ren, C. J. Sheils, P. L. Paris, D. C. Tahmassebi and E. T. Kool, *J. Am. Chem. Soc.*, 1996, **118**, 8182.
39 L. S. Lerman, *J. Mol. Biol.*, 1961, **3**, 18.
40 S. K. Burley and G. A. Petsko, *Science*, 1985, 23.
41 C. A. Hunter, *Chem. Soc. Rev.*, 1994, **23**, 101.
42 S. B. Ferguson and F. Diederich, *Angew. Chem., Int. Ed. Engl.*, 1986, **25**, 1127.
43 D. B. Smithrud and F. Diederich, *J. Am. Chem. Soc.*, 1990, **112**, 339.
44 R. E. Sheridan and H. W. Whitlock, *J. Am. Chem. Soc.*, 1988, **110**, 4071.
45 B. J. Whitlock and H. W. Whitlock, *J. Am. Chem. Soc.*, 1990, **112**, 3910.
46 T. J. Shepodd, M. A. Petti and D. A. Dougherty, *J. Am. Chem. Soc.*, 1988, **110**, 1983.
47 A. W. Schwabacher, S. Zhang and W. Davy, *J. Am. Chem. Soc.*, 1993, **115**, 6995.
48 H. J. Schneider, T. Blatter, S. Simova and I. Theis, *J. Chem. Soc., Chem. Commun.*, 1989, 580.
49 A. D. Hamilton and D. Van Engen, *J. Am. Chem. Soc.*, 1987, **109**, 5035.
50 A. V. Muehldorf, D. Van Engen, J. C. Warner and A. D. Hamilton, *J. Am. Chem. Soc.*, 1988, **110**, 6561.
51 J. Rebek, Jr. and D. Nemeth, *J. Am. Chem. Soc.*, 1986, **108**, 5637.
52 J. Rebek, Jr., B. Askew, P. Ballester, C. Buhr, S. Jones, D. Nemeth and K. Williams, *J. Am. Chem. Soc.*, 1987, **109**, 5033.
53 C. W. Chen and H. W. Whitlock, *J. Am. Chem. Soc.*, 1978, **100**, 4921.
54 S. C. Zimmerman and C. M. Vanzyl, *J. Am. Chem. Soc.*, 1987, **109**, 7894.
55 S. C. Zimmerman, C. M. Vanzyl and G. S. Hamilton, *J. Am. Chem. Soc.*, 1989, **111**, 1373.
56 S. C. Zimmerman, K. W. Saionz and Z. J. Zeng, *Proc. Natl. Acad. Sci.*, 1993, **90**, 1190.
57 S. C. Zimmerman and K. W. Saionz, *J. Am. Chem. Soc.*, 1995, **117**, 1175.
58 S. C. Zimmerman, F. W. Zeng, D. E. C. Reichert and S. V. Kolotuchin, *Science*, 1996, **271**, 1095.
59 R. P. Sijbesma, A. P. M. Kentgens and R. J. M. Nolte, *J. Org. Chem.*, 1991, **56**, 3199.
60 J. N. H. Reek, A. H. Priem, H. Engelkamp, A. E. Rowan, J. Elemans and R. J. M. Nolte, *J. Am. Chem. Soc.*, 1997, **119**, 9956.
61 M. Crego, C. Raposo, C. M. Caballero, E. Garcia, J. G. Saez and J. R. Moran, *Tetrahedron Lett.*, 1992, **33**, 7437.
62 J. S. Zhang and J. S. Moore, *J. Am. Chem. Soc.*, 1992, **114**, 9701.
63 A. S. Shetty, J. S. Zhang and J. S. Moore, *J. Am. Chem. Soc.*, 1996, **118**, 1019.
64 Y. Tobe, N. Utsumi, A. Nagano and K. Nemaemura, *Angew. Chem., Int. Ed. Engl.*, 1988, **37**, 1285.
65 J. C. Nelson, J. G. Saven, J. S. Moore and P. G. Wolynes, *Science*, 1997, **277**, 1793.
66 R. S. Lokey and B. L. Iverson, *Nature*, 1995, **375**, 303.
67 R. S. Lokey, Y. Kwok, V. Guelev, C. J. Pursell, L. H. Hurley and B. L. Iverson, *J. Am. Chem. Soc.*, 1997, **119**, 7202.
68 L. F. Newcomb and S. H. Gellman, *J. Am. Chem. Soc.*, 1994, **116**, 4993.
69 L. F. Newcomb, T. S. Haque and S. H. Gellman, *J. Am. Chem. Soc.*, 1995, **117**, 6509.
70 Y. P. Pang, J. L. Miller and P. A. Kollman, *J. Am. Chem. Soc.*, 1999, **121**, 1717.
71 N. J. Heaton, P. Bello, B. Herrandon, A. del Campo and J. Jimenez-Barbero, *J. Am. Chem. Soc.*, 1998, **120**, 12371.
72 G. A. Breault, C. A. Hunter and P. C. Mayers, *J. Am. Chem. Soc.*, 1998, **120**, 3402.
73 D. B. Smithrud, E. M. Sanford, I. Chao, S. B. Ferguson, D. R. Carcanague, J. D. Evanseck, K. N. Houk and F. Diederich, *Pure Appl. Chem.*, 1990, **62**, 2227.
74 B. L. Allwood, N. Spencer, H. Shahriari-Zavereh, J. F. Stoddart and D. J. Williams, *J. Chem. Soc., Chem. Commun.*, 1987, 1064.
75 P. R. Ashton, T. T. Goodnow, A. E. Kaifer, M. V. Reddington, A. M. Z. Slawin, N. Spencer, J. F. Stoddart, C. Vicent and D. J. Williams, *Angew. Chem., Int. Ed. Engl.*, 1989, **28**, 1396.
76 D. B. Amabilino, P. R. Ashton, S. E. Boyd, J. Y. Lee, S. Menzer, J. F. Stoddart and D. J. Williams, *Angew. Chem., Int. Ed. Engl.*, 1997, **36**, 2070.
77 P. R. Ashton, M. Grognuz, A. M. Z. Slawin, J. F. Stoddart and D. J. Williams, *Tetrahedron Lett.*, 1991, **32**, 6235.
78 D. B. Amabilino, P. R. Ashton, C. L. Brown, E. Cordova, L. A. Godinez, T. T. Goodnow, A. E. Kaifer, S. P. Newton, M. Pietraszkiewicz, D. Philp, F. M. Raymo, A. S. Reder, M. T. Rutland, A. M. Z. Slawin, N. Spencer, J. F. Stoddart and D. J. Williams, *J. Am. Chem. Soc.*, 1995, **117**, 1271.
79 F. Cozzi, M. Cinquini, R. Annunziata, T. Dwyer and J. S. Siegel, *J. Am. Chem. Soc.*, 1992, **114**, 5729.
80 F. Cozzi, M. Cinquini, R. Annunziata and J. S. Siegel, *J. Am. Chem. Soc.*, 1993, **115**, 5330.
81 F. Cozzi, F. Ponzini, R. Annunziata, M. Cinquini and J. S. Siegel, *Angew. Chem., Int. Ed. Engl.*, 1995, **34**, 1019.

82 S. Paliwal, S. Geib and C. S. Wilcox, *J. Am. Chem. Soc.*, 1994, **116**, 4497.
83 E. Kim, S. Paliwal and C. S. Wilcox, *J. Am. Chem. Soc.*, 1998, **120**, 11192.
84 L. Serrano, M. Bycroft and A. R. Fersht, *J. Mol. Biol.*, 1991, **218**, 465.
85 H. Adams, F. J. Carver, C. A. Hunter, J. C. Morales and E. M. Seward, *Angew. Chem.*, *Int. Ed. Engl.*, 1996, **35**, 1542.
86 F. J. Carver, C. A. Hunter and E. M. Seward, *Chem. Commun.*, 1998, 775.
87 C. A. Hunter and X. J. Lu, *J. Mol. Biol.*, 1997, **265**, 603.
88 M. J. Packer, M. P. Dauncey and C. A. Hunter, *J. Mol. Biol.*, 2000, **295**, 71.
89 M. J. Packer, M. P. Dauncey and C. A. Hunter, *J. Mol. Biol.*, 2000, **295**, 85.
90 P. L. Anelli, N. Spencer and J. F. Stoddart, *J. Am. Chem. Soc.*, 1991, **113**, 5131.
91 R. A. Bissell, E. Cordova, A. E. Kaifer and J. F. Stoddart, *Nature*, 1994, **369**, 133.
92 For a recent review of this field, see M. R. Bryce, *Adv. Mater.*, 1999, **11**, 11.
93 G. W. Coates, A. R. Dunn, L. M. Henling, D. A. Dougherty and R. H. Grubbs, *Angew. Chem.*, *Int. Ed. Engl.*, 1997, **36**, 248.
94 H. C. Kolb, P. G. Andersson and K. B. Sharpless, *J. Am. Chem. Soc.*, 1994, **116**, 1278.